MATCHED FILTER QRS DETECTION

A Thesis

Submitted to

The Faculty of Graduate Studies

of

The University of Manitoba

In Partial Fulfilment

of the Requirements

for the Degree

Master of Science

Department of Electrical Engineering

J. Russell Storry

August, 1977

MATCHED FILTER QRS DETECTION

by

J. Russell Storry

A dissertation submitted to the Faculty of Graduate Studies of the University of Manitoba in partial fulfillment of the requirements of the degree of

Master of Science

ABSTRACT

Principles of signal detection theory are used to develop and test a more reliable method of detecting the electrocardiograph signal (PQRST wave) corresponding to a heart beat in the presence of interfering muscle and artifact noise. The improved method uses a matched filter specified by the parameters of the heart signal and the interfering noise. Experimental tests show that the matched filter QRS detector exhibits a performance improvement over two existing detection methods. The matched filter QRS detector also demonstrates the property of robustness in experimental signal parameter sensitivity tests.

TABLE OF CONTENTS

(TABLE OF CONTENTS continued)

LIST OF FIGURES

(LIST OF FIGURES - continued)

(LIST OF FIGURES - continued)

LIST OF TABLES

ACKNOWLEDGEMENTS

I wish to thank my advisor and friend, Professor Ed Shwedyk for suggesting this topic and for his enthusiastic support throughout the course of the work. The technical facilities and financial aid provided by the University are also greatly appreciated. For the capable and patient typing of this thesis by Shelagh Hallson, I express a heartfelt thank you.

CHAPTER I

INTRODUCTION

Detection of the human heart's electrical signal is required by many measurements in health care and health care related fields. One very common application of electrical heart signal detection is to measure heart rate. Another less common application is to provide timing for the averaging method of ECG (electrocardiograph) signal recovery in the presence of noise.

Even the simplest electrode based heart rate measurement devices contain circuitry to detect electrical heart signals. This device or circuit module is called a QRS detector. The function of the QRS detector is to detect the QRS complex portion of the heart signal indicating the occurrence of a heart beat (Fig. 1.1). The QRS detector is usually preceded by a high gain preamplifier that amplifies the significant heart signal (0.5 Hz to 50 Hz) from 1 mV p-p to 1 V p-p. The QRS detector is then followed by circuitry that calculates and displays heart rate. Fig. 1.2 illustrates the block diagram of such a heart rate meter.

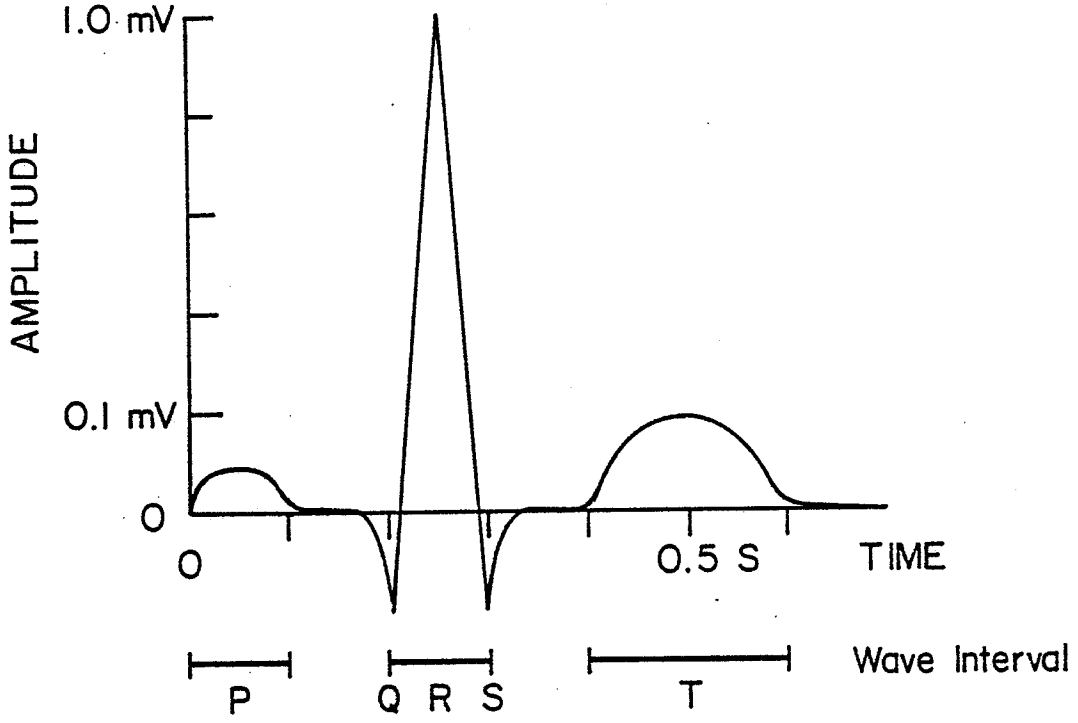

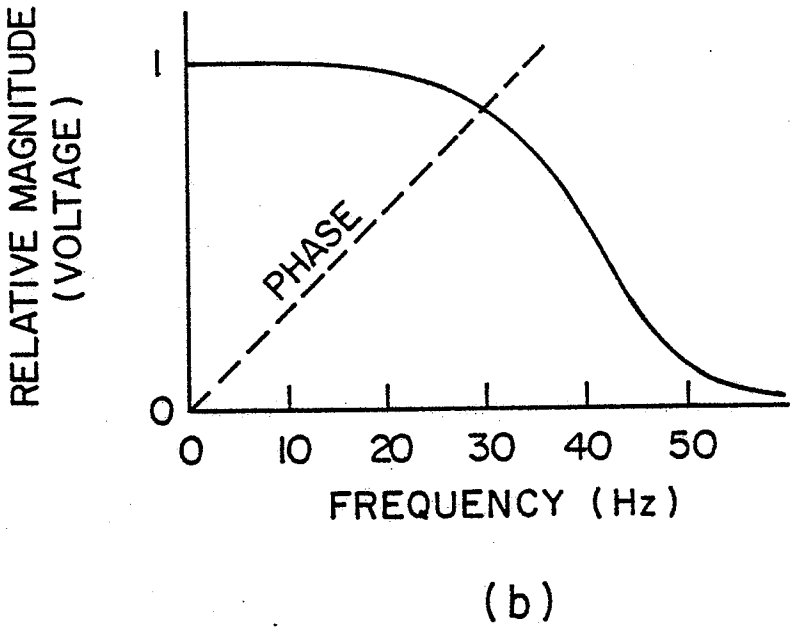

Fig. 1.1 Typical PQRST wave;
(a) in time domain,
(b) in frequency domain (linear phase)

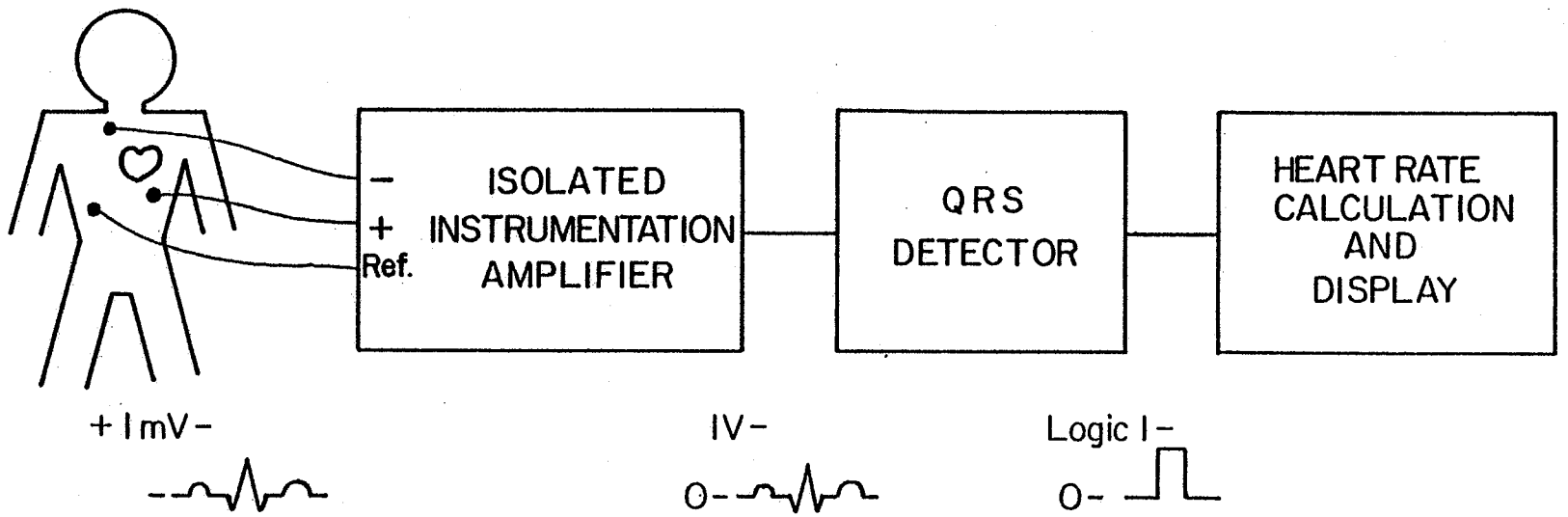

Fig. 1.2 Typical heart beat meter configuration.

1.1 QRS Detector Performance Considerations

The ability of the QRS detector to trigger reliably, that is, without extra or missed triggers is often the main factor controlling the accuracy of a heart beat meter, assuming good surface electrode application and location as well as proper preamplifier design. Wrong decisions made by the QRS detector cause incorrect heart beat readings that are usually interpreted by the user as false or missed beats, indicated by physiologically unlikely sharp increases or decreases in heart rate. The magnitude of these sudden changes depends on the dynamics of the heart rate calculation circuitry. When this type of indication occurs, confidence in the accuracy and reliability of the heart rate measurement is reduced. Similarly, if heart rate is being monitored remotely using a high-low heart rate sensor, detection errors will cause needless false alarms. In ECG signal averaging applications, recovery is very sensitive to false triggers as they impair signal to noise enhancement of the recovered signal.

False beats and extra beats erroneously detected in a healthy subject are caused by interfering noise inseparably added to the heart signal within the body and at the skin to electrode interface. Interfering EMG (electromyograph) signals are generated within the body when muscles are active, while movement artifact noise is generated by skin to electrode voltaic cell potential disruption caused by electrode movement

relative to the skin. Interference from 60Hz noise is assumed to be eliminated by proper instrumentation design. A typical sample of muscle and artifact noise are shown in both the time and frequency domain in Fig. 1.3.

Extra beats are also caused by false triggering on high T waves when the T wave is not included in the total signal being detected. This allows simpler detection schemes with a performance penalty. Ideally, the detector should look for the presence of a PQRST wave. When a QRS detector is referred to in this thesis, full PQRST detection is implied.

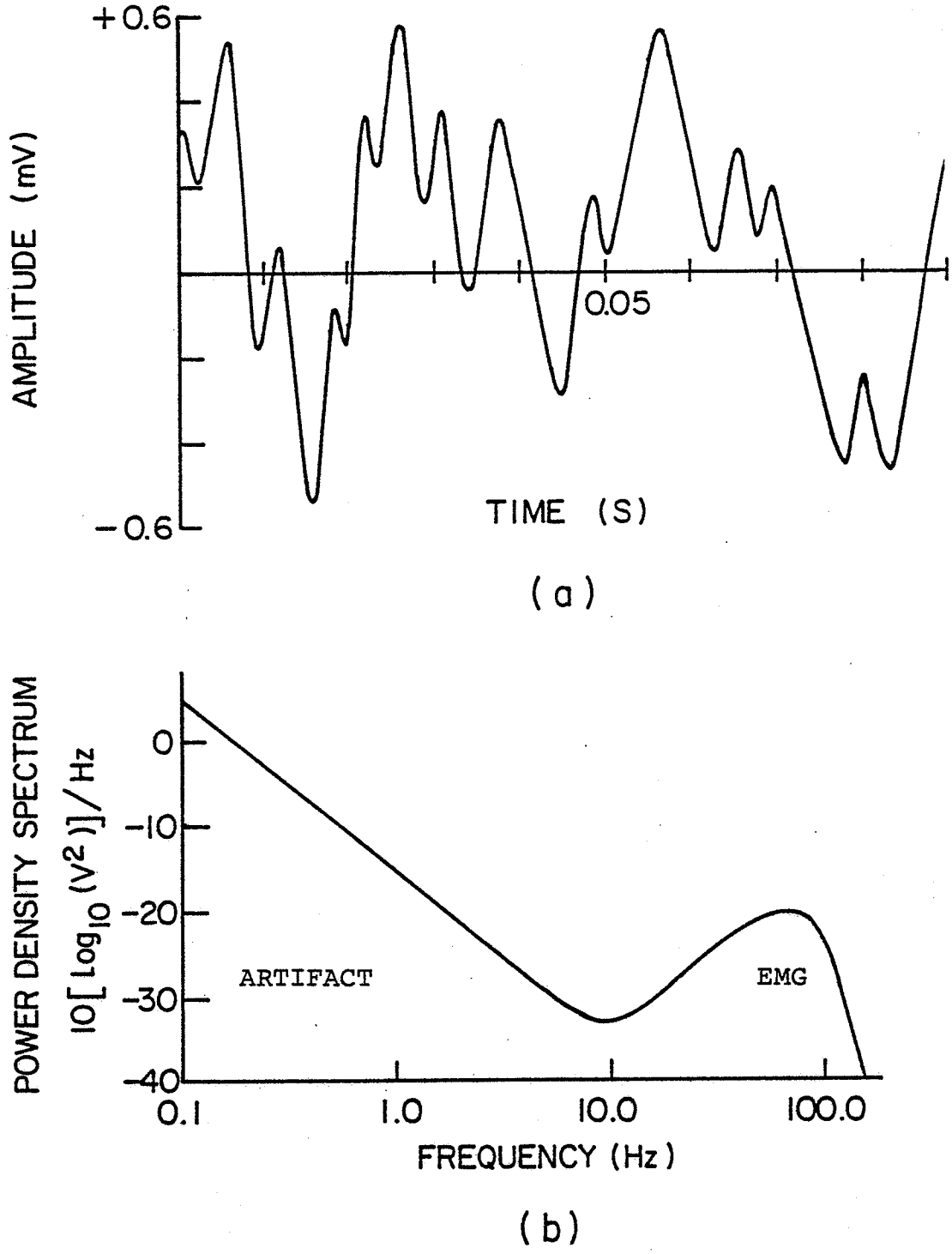

Fig. 1.3 Typical EMG and artifact noise;
(a) time domain;
(b) power density spectrum

1.2 Present QRS Detection Methods and Proposed Scheme

The most direct way to reduce QRS detection errors is to maintain the subject at rest. Under these conditions, simple and reliable QRS detectors are easily realized (Fig. 1.4).

When the subject is active as in exercise testing, the approach to QRS detection in Fig. 1.4 is not reliable. To increase reliability circuit designers have added extra signal processing to eliminate false and missed triggers due to noise. Analogue and digital techniques involving squaring, differentiating, automatic threshold setting, full wave rectification, hi-Q band pass filtering and other operations are utilized in various combinations to improve QRS detection in the presence of muscle and artifact noise. Examples of some complex QRS detectors taken from [1] and [2] are shown in Fig. 1.5.

By controlling the type of physical activity, using good electrode placement and carefully adjusting these detectors to suit the subject, reasonably reliable heart beat detection can be achieved. Usually, the more reliable the detector, the greater the initial adjustment required by the user. From the user's viewpoint, the ideal QRS detector would perform as well during exercise as during rest, independent of exercise type, with any electrode lead system and without any adjustment. The answer as to whether such an ideal QRS detector is possible lies in determining the structure of the optimum detector and evaluating its performance. The key to determine the optimum structure lies in signal detection theory.

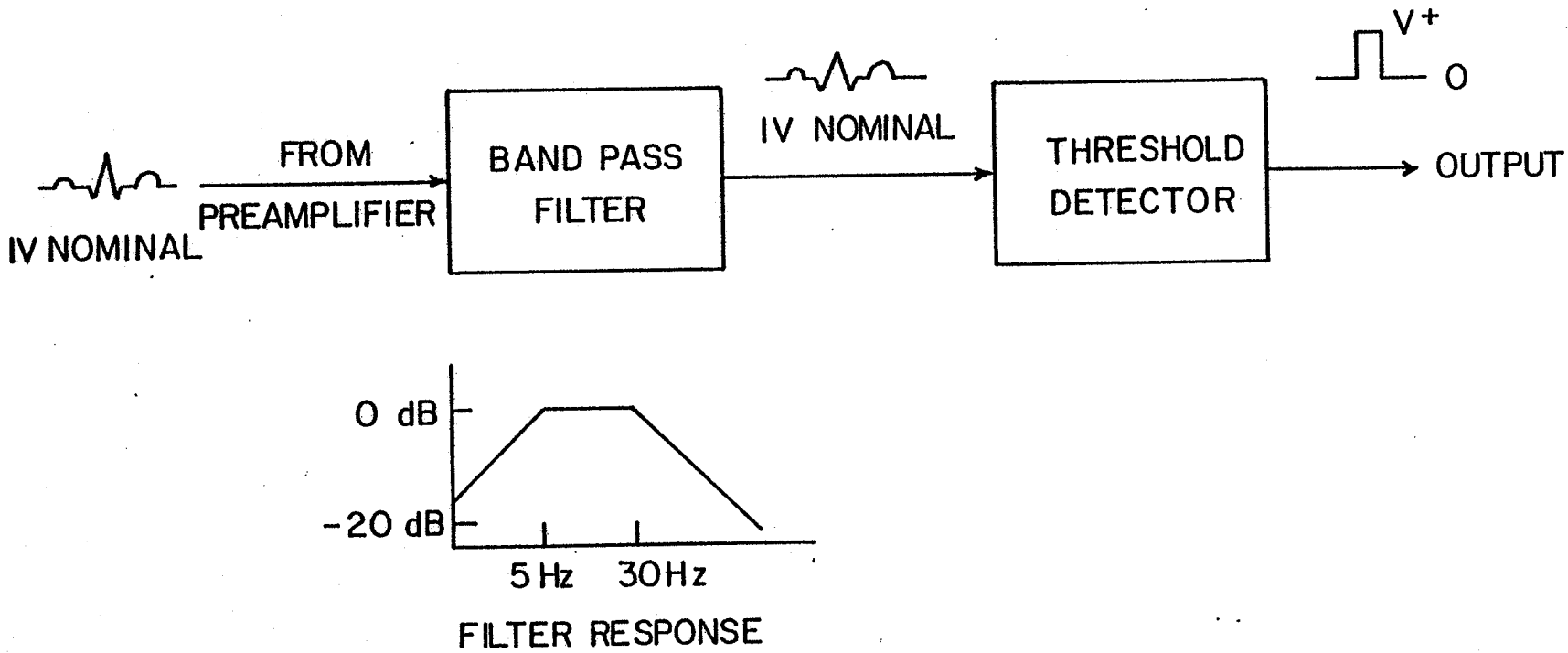

Fig. 1.4 Simple QRS detector

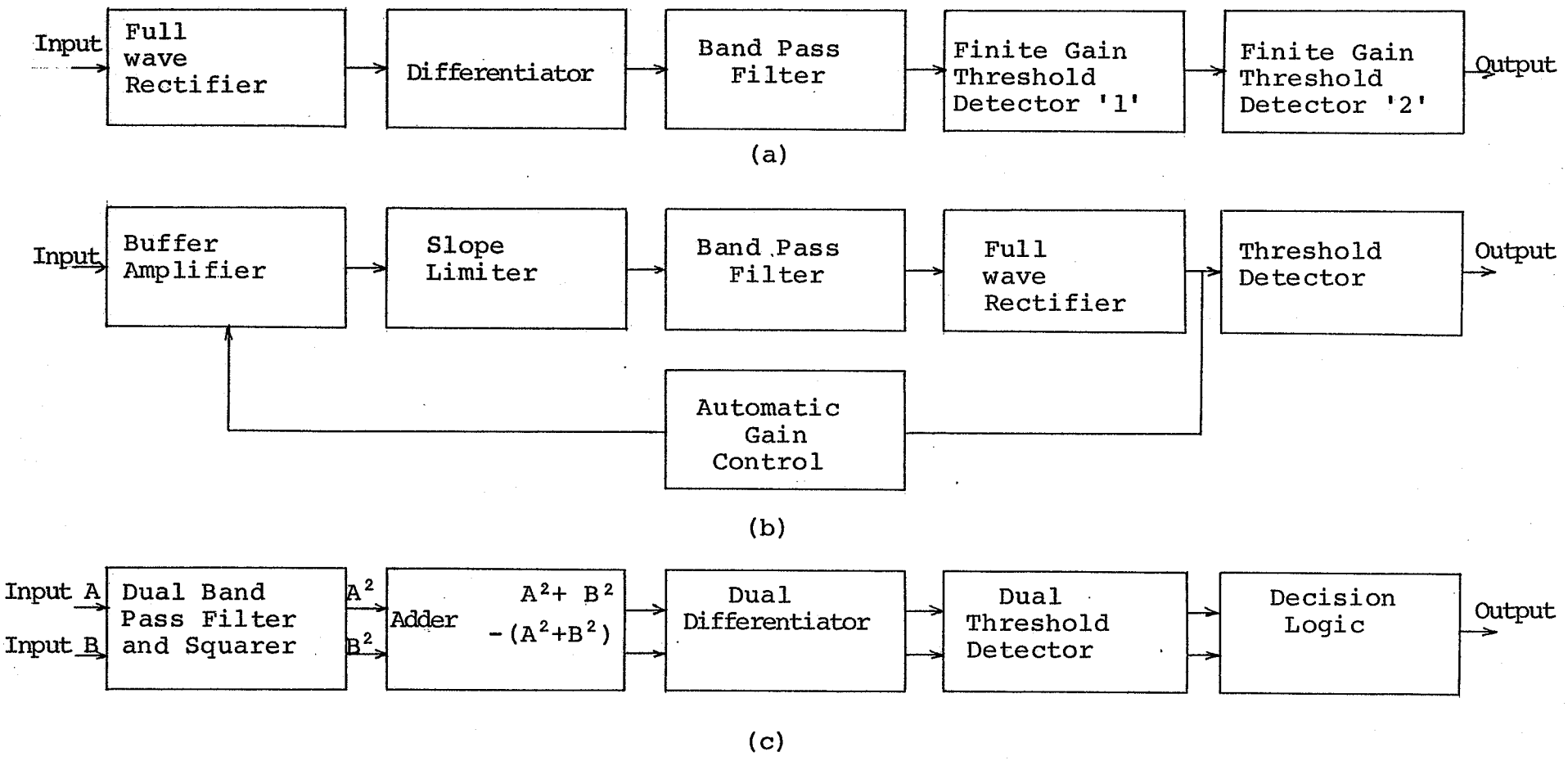

Fig. 1.5 Complex QRS detector schemes. (a) and (b) are taken from [1] while (c) is taken from [2].

It is theoretically suggested and well verified in practice that the structure of the optimal linear device for detecting a known signal in white noise with minimum probability of error uses a matched filter (Fig. 1.6). In addition, if the noise is Gaussian, the matched filter detector is optimum for both linear and nonlinear systems. If the noise is not Gaussian, the matched filter while still part of the optimum linear detector, may not perform as well as some nonlinear detectors. In practice, matched filter systems are usually quite robust, even in non-Gaussian noise situations [3].

The matched filter has been used in computer aided ECG evaluation programs to locate QRS complexes off line by correlation [4]. This procedure does not include pre-whitening by the PDS (power density spectrum) of the noise. Therefore, the interfering noise was assumed to be white. For example, Hambly et al [5] used a matched filter QRS complex locator as a component of their noise reducing ECG filter, based on the structure suggested by estimation theory for minimum MSE (mean square error) signal recovery from noise.

In a similar manner, this thesis uses signal detection theory to develop an optimal QRS detector. The filter is realized in real time and then experimentally evaluated by comparison with existing QRS detectors. Research into the particular aspects and practical consequences of applying detection theory to the engineering problem of reliable QRS detection during exercise is presented.

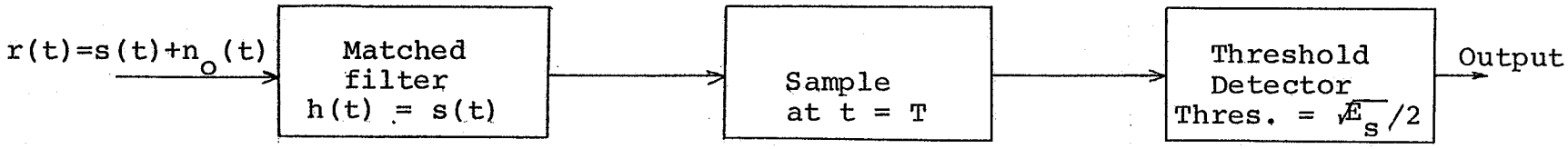

$s(t) = 0, \quad t < 0, \; t > T$

Fig. 1.6 Matched filter receiver for detecting the equally likely occurrence of $s(t) + n_o(t)$ or $n_o(t)$ only.

CHAPTER II

ASPECTS OF OPTIMUM QRS DETECTION DESIGN

2.1 Introduction

The design of an optimum receiver for a specific application in signal detection requires a knowledge of the statistical and the deterministic properties of both the signal and the noise involved. An engineering model can then be developed based on the available signal parameters and on the worst case assumptions for the essential unavailable parameters. The model must adequately represent the problem so that the applicable theory will lead to a realizable solution with predictable performance.

The deterministic and statistical properties of the ECG signal, EMG and artifact noise on which to base the engineering model are readily available in the literature [6-10]. The detection theory principles subsequently applied are well known. The comprehensive text "Detection, Estimation and Modulation Theory" Part I by H.L. Van Trees is the main source of analysis for the solution of the modeled problem [11].

2.2 Modeling Surface Electrode Signals

The typical surface electrode heart signal presented in Fig. 1.1 is one of a set of similar signals that can vary greatly from subject to subject despite consistent lead placement and standard instrumentation. Variation of the measurement conditions of one subject generates additional subsets of heart signals. The six and twelve multiple lead systems used in clinical ECG diagnosis shown in Fig. 2.1 demonstrate the variability in signal shapes of the different leads for one individual. It is also well established that the heart signal varies with heart rate [12]. For a given lead configuration, the heart signal at 180 BPM (beats per minute) is not the same as the nominal 60 BPM rest heart signal (Fig. 2.2). The task of a deterministic description of the complete set of heart signals with as few parameters as possible is formidible.

In this thesis, a single lead from one subject at rest was used for a low rate heart signal. The same single lead from another subject was used to create a 180 BPM signal s(t) from the rest heart rate using the empirical correction factors suggested in [12]. The lead placement and heart signals used are shown in Fig. 2.3. This amounts to choosing only two signals to represent the complete set. The strategy here is to assume the optimum detector is not sensitive to the shape of the heart signal. If sensitivity is a problem, then the detector is assumed to have the facility to learn the shape

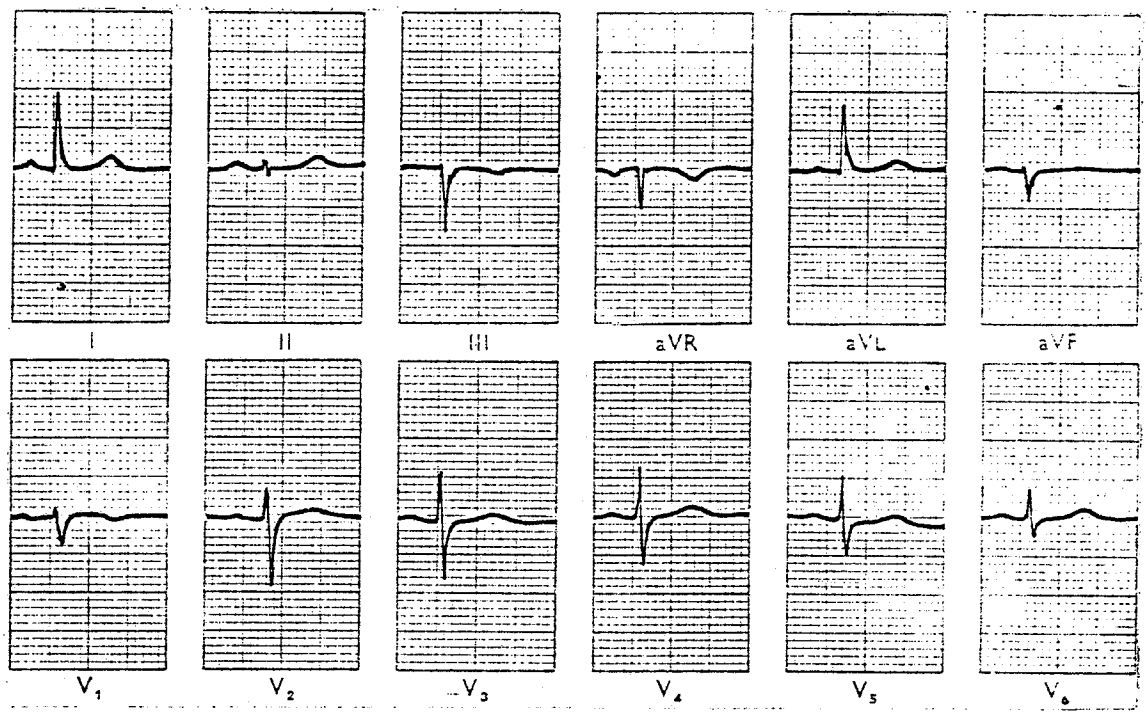

Fig. 2.1 Multiple lead clinical ECG.

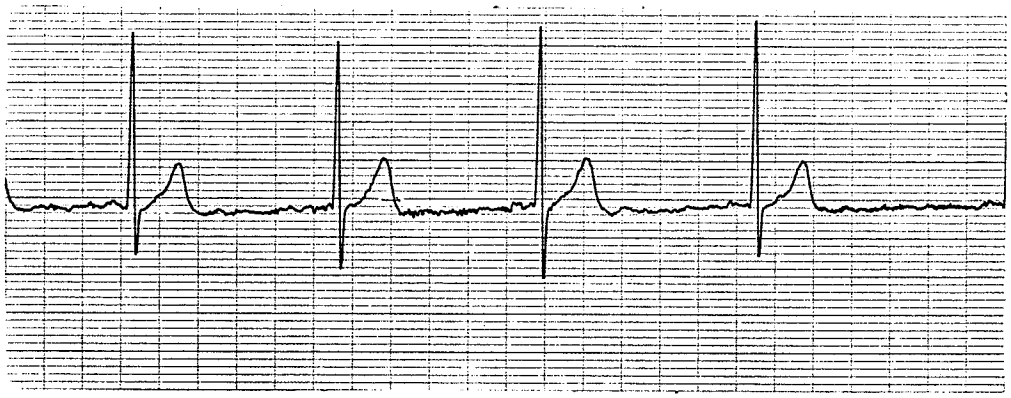

(a) Rest heart rate

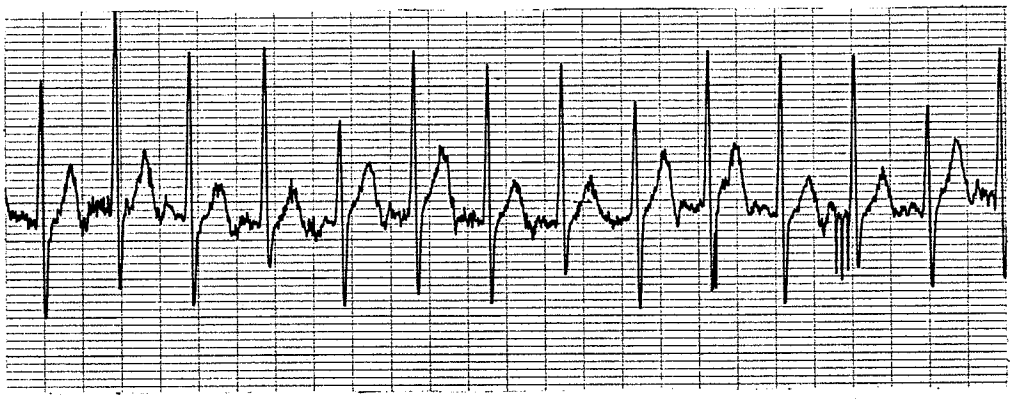

(b) Maximum heart rate

Fig. 2.2 Rest rate and maximum rate heart signal, same subject, same lead.

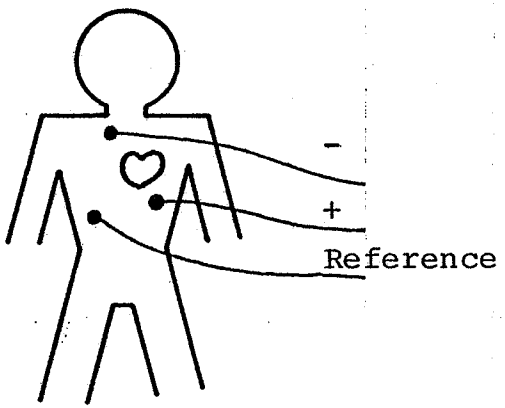

(a) 70 BPM reference heart signal

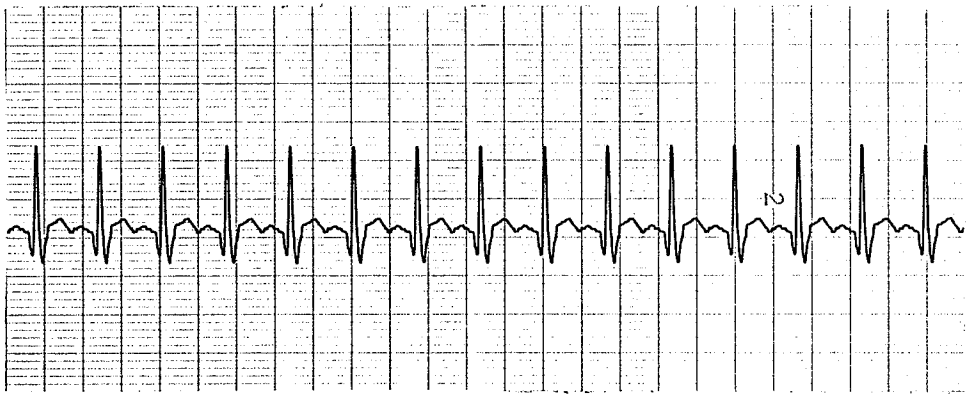

(b) 180 BPM reference heart signal

Fig. 2.3 Reference heart signals and lead configuration.

of the particular heart signal being detected. The heart signal is modeled as a known repetitive signal with random time intervals of occurrence.

The surface electrode EMG noise is modeled as quasi-stationary Gaussian noise with a rational PDS taken from the results of [9] and specified as follows (Fig. 2.4).

$$N_{emg}(f) = \frac{N_0 f^2}{1508.25 \left(\frac{f^2}{55^2}+1\right)\left(\frac{f^4}{100^4}+1\right)} \quad V^2/Hz \qquad (2.1)$$

The quasi-stationary property is based on the assumption that the shape of the PDS does not vary with changes in instantaneous power or variance. As it turns out, the structure of the optimum detector depends only on the PDS shape and not on the variance. Therefore, quasi-stationarity eliminates the need for a time varying structure requiring continuous noise parameter estimation. The accuracy of the noise PDS shape required depends on the sensitivity of the detector's performance to PDS change. Since the spectrum is assumed to be rational, the EMG noise can be generated by passing white Gaussian noise through a linear filter with a transfer function H(f) such that

$$H(f) \times H^*(f) = \frac{kf^2}{\left(\frac{f^2}{55^2}+1\right)\left(\frac{f^4}{100^4}+1\right)} \quad V/Hz \qquad (2.2)$$

It is well known [11] that if the input to a linear system is Gaussian then the output is Gaussian. An EMG

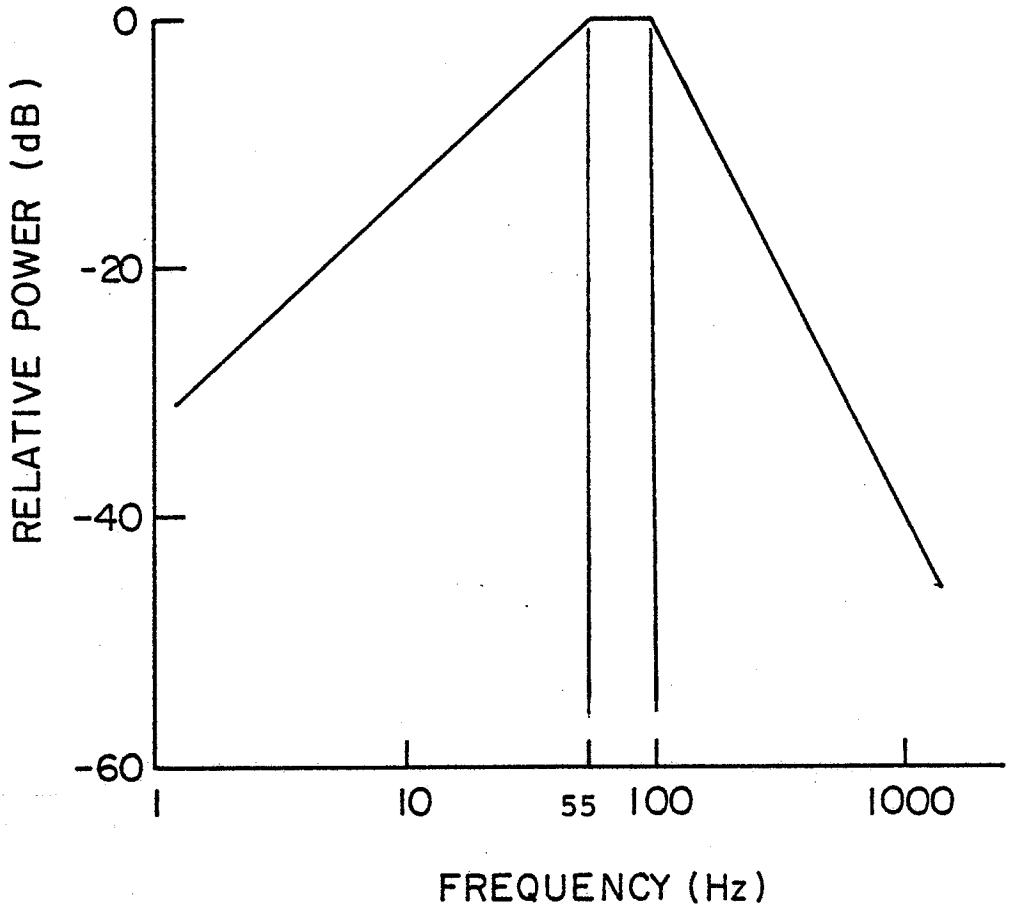

Fig. 2.4 Bode Approximation of EMG PDS

simulation scheme utilizing this fact is illustrated in Fig. 2.5.

The model for surface electrode artifact noise is based on work by Winter et al [2,10]. All that is assumed to be known about the artifact noise is its PDS, N_{art}.

$$N_{art}(f) = \frac{k}{f^2} \qquad V^2/Hz \qquad (2.3)$$

Artifact noise is generated by passing Gaussian noise through a 1 Hz single pole low pass active filter to approximate the frequency domain specification of equation 2.3 above 1 Hz. The amplitude distribution of artifact noise is chosen to be Gaussian.

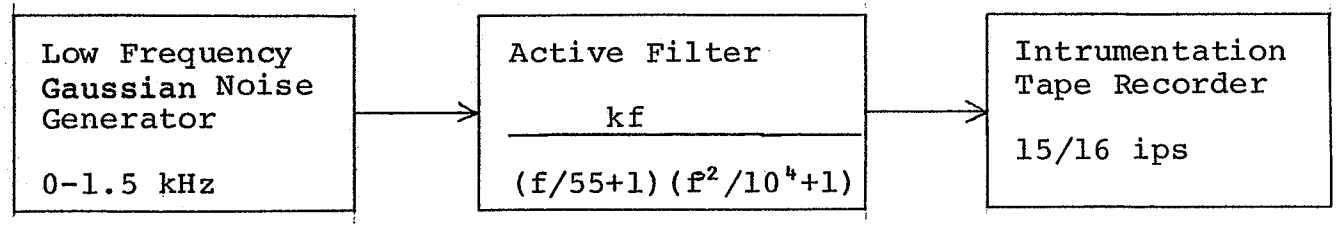

Fig. 2.5 Stationary EMG Noise Simulation

2.3 Engineering Solution of Optimal Heart Signal Detection

The ECG, EMG and artifact signals modeled individually can be combined into one model as shown in Fig. 2.6. A white noise source N_o is added to represent the noise contribution of the devices used in the system realization. The EMG, artifact and white noise have a combined PDS (Fig. 2.7) that corrupt the heart signal s(t) before detection. The problem is to determine if s(t) is contained in the received signal r(t).

$$r(t) = s(t) + n(t) \qquad (2.4)$$

$$\text{or} \quad r(t) = n(t) \qquad (2.5)$$

$$\text{where} \quad n(t) = N_o(t) + N_{emg}(t) + N_{art}(t) \qquad (2.6)$$

A filter that responds minimally to the noise energy and maximally to the signal energy will permit the most accurate threshold detector decision as to whether the signal is present. The filter that provides the greatest possible signal power to noise power improvement before threshold detection will exhibit the optimum performance (Fig. 2.8).

The NPO (noise power output) of a linear filter with frequency domain specification H(f) is

$$NPO = \int_{-\infty}^{\infty} N(f) |H(f)|^2 df \qquad V^2/\Omega \qquad (2.7)$$

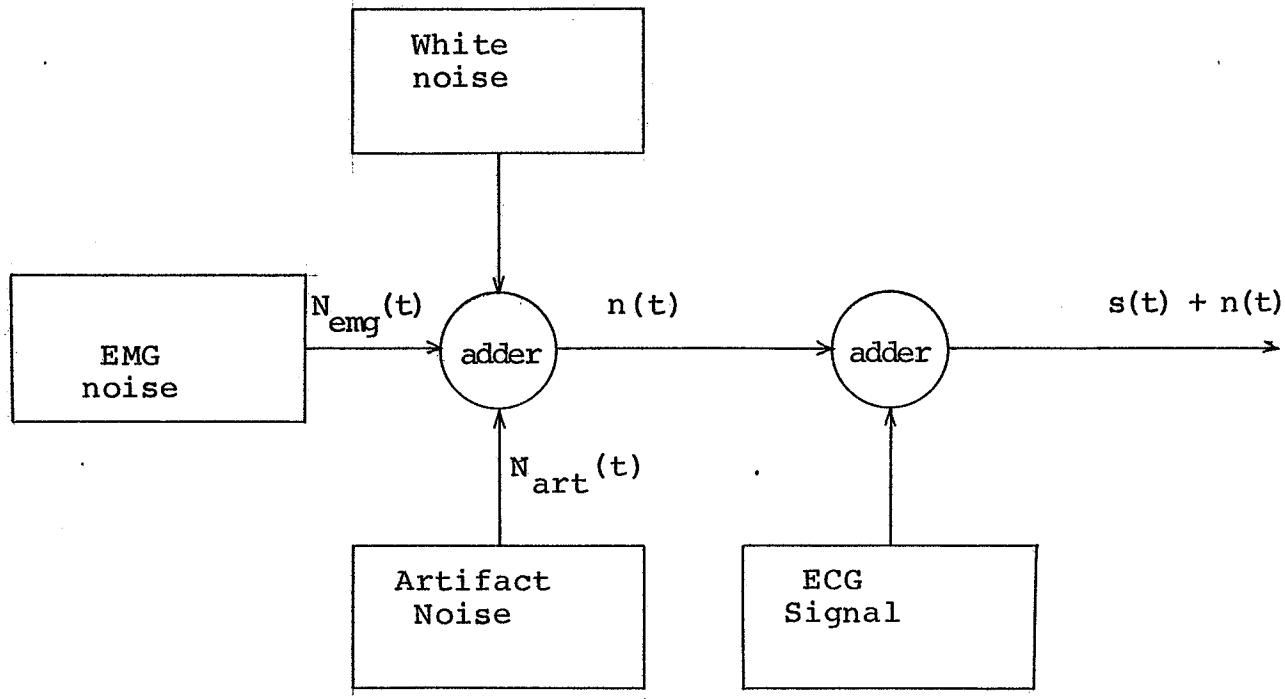

Fig. 2.6 Model for simulating Noisy ECG signals

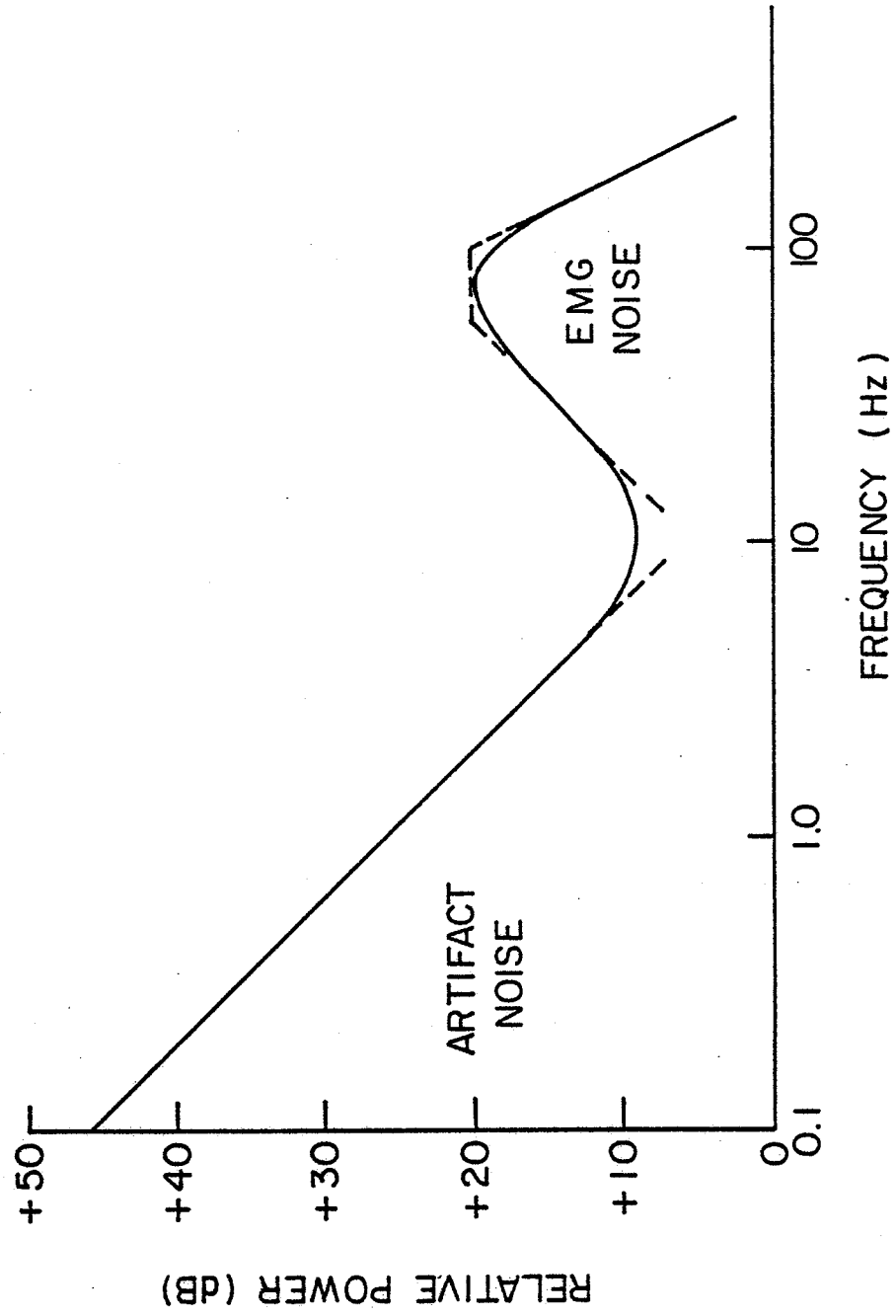

Fig. 2.7 Bode Approximation of Total Noise PDS

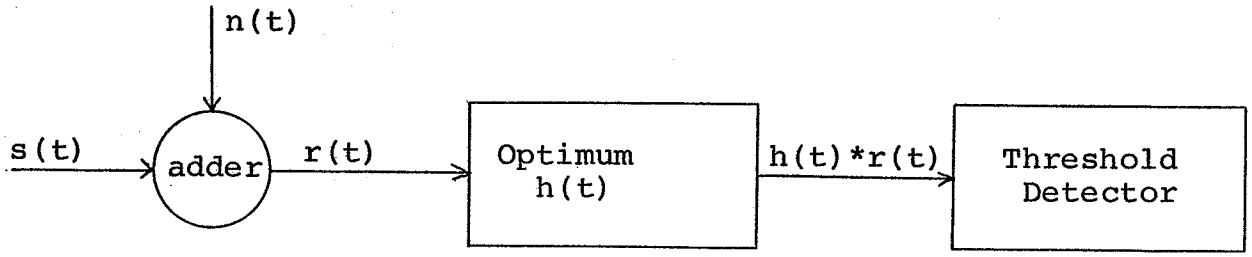

Fig. 2.8 Basic, Matched filter QRS Detector.
(Optimum h(t) maximizes $\overline{[h(t)*s(t)]}^2/\overline{[h(t)*n(t)]^2}$)

Similarly, the SPO (signal power out) is,

$$SPO = \int_{-\infty}^{\infty} |S(f)\ H(f)|^2 df \qquad V^2/1\Omega \qquad (2.8)$$

The signal to noise ratio at the output is then,

$$S/N = \frac{\int_{-\infty}^{\infty} |S(f)\ H(f)|^2 df}{\int_{-\infty}^{\infty} |N(f)|^2 |H(f)|^2 df} \qquad V^2/V^2 \qquad (2.9)$$

It is shown in Van Trees [11] that S/N is maximized when

$$\int_{t_i}^{t_f} k(t-u)\ h(u)\ du = s(t) \qquad t_i \leq t \leq t_f \qquad (2.10)$$

where $k(\alpha)$ is the autocorrelation function of the total noise $N(t)$; t_i and t_f define the observation interval of the detector. Equation 2.10 is an integral equation that must be solved to determine $h(t)$. Assuming an infinite observation interval, this equation may be solved using Fourier transformations as follows:

$$k(t) * h(t) = s(t) \qquad (2.11)$$

or

$$H(f) = \frac{S(f)}{|N(f)|^2} \qquad (2.12)$$

The observation interval may be considered infinite if the minimum successive signal occurrence interval is greater than the FIR (finite impulse response) of a reasonably truncated optimum filter. When the optimum FIR time is less than the minimum interval between signal occurrence, a method to solve 2.11 is by discretization into matrix form to provide the numerical solution for h(t).

Since specific heart signals cannot be expressed in a closed analytic form, 2.12 must be evaluated numerically. The known heart signal is discretized and transformed to the discrete frequency domain. The discrete form of $|N(f)|^2$ is divided point by point into S(f) and the result transformed back to the time domain to yield a discrete optimum h(t). A procedural flow chart is shown in Fig. 2.9 including details of computer hardware and software required. Appendix A contains a detailed explanation of the procedures referred to in Fig. 2.9.

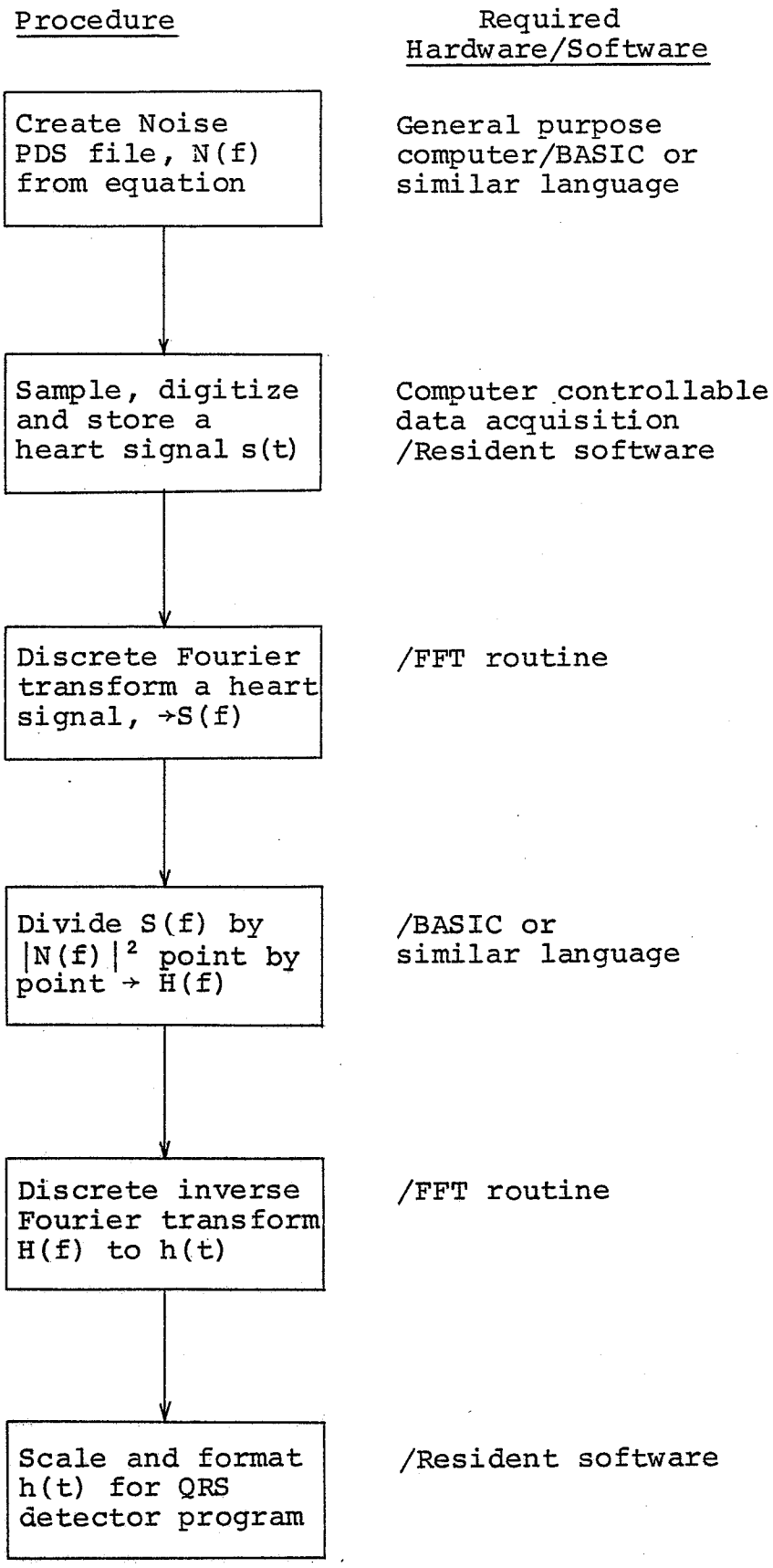

Fig. 2.9 Calculation of optimum h(t)

2.4 Optimum Detector Realization

The optimum h(t) in Fig. 2.9 does not lend itself to analogue filter synthesis. However, the filter can be directly implemented using a digital FIR transversal filter. Fig. 2.10 indicates the block diagram of the digital implementation using a 16 bit minicomputer equipped with a software controlled data acquisition system. The 250 Hz sampling rate and 16 bit word lengths used are overspecified to the maximum allowable on the particular minicomputer available. Using this 'too much is enough' strategy, discretization and computation error minimally degrade the optimum detector's performance. If worthwhile performance is established, then the minimum sampling rate and word lengths that simplify structure while maintaining performance may be investigated.

Having developed a method to design and to implement an optimum detector for the given assumptions, the next possibility is to compare and evaluate its performance with heart beat detectors now in use as well as determine the optimum detector's sensitivity to assumed signal and noise parameter variations. The performance evaluation may be done analytically, numerically or experimentally. The experimental method is the most direct means of comparative testing and eliminates the need to model existing detectors. The specification and method of experimental performance evaluation is the subject of the next chapter.

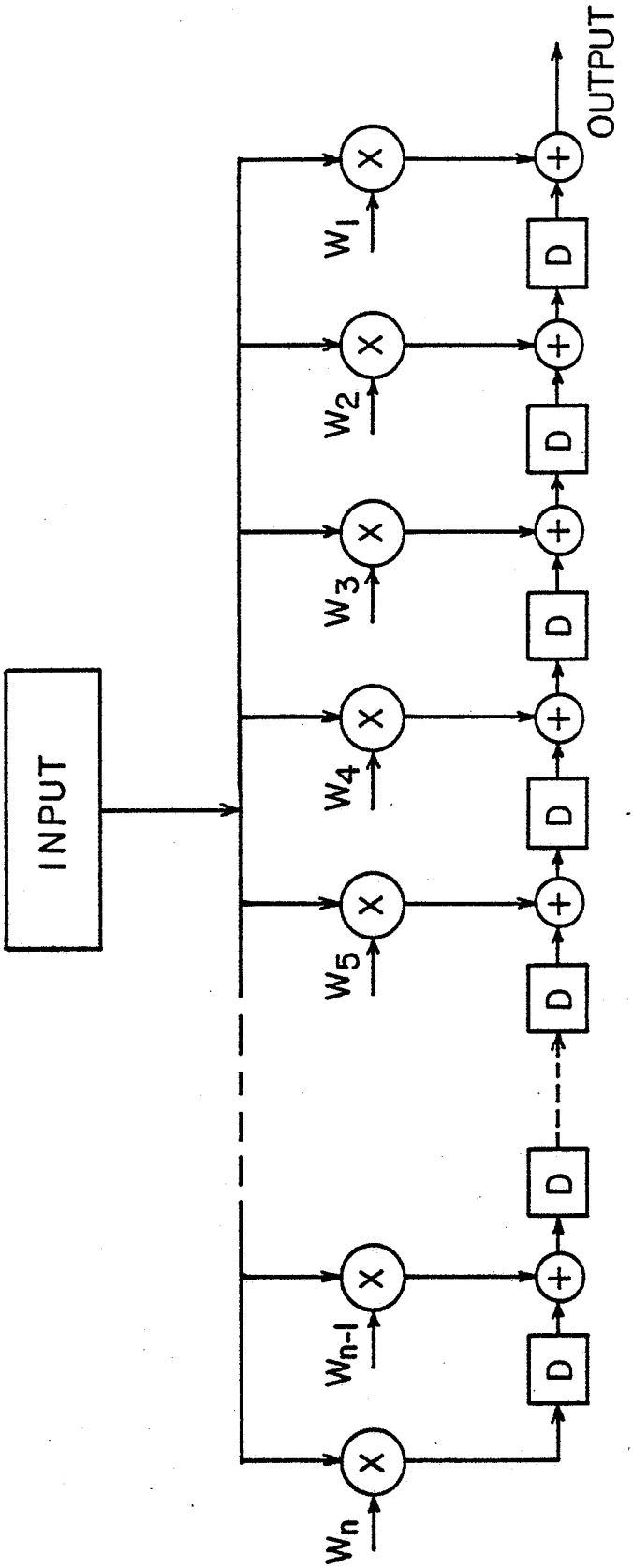

Fig. 2.10 Digital FIR transversal filter implementation

CHAPTER III

QRS DETECTOR EVALUATION TECHNIQUE

3.1 Introduction

In the past, QRS detection evaluation was performed by using an actual noisy record that has been interpreted for the total number of heart beat occurrences. It is a quick, but rather subjective test. The performance testing technique used in this thesis is more exhaustive and quantitative. However, it is more time consuming and its meaningfulness limited by the accuracy of the signal models used. If the modeling and simulation are adequate, performance improvement predicted by exhaustive testing should be evident in conventional subjective tests.

Quantitative evaluation and comparison of QRS detectors require a more exact measure of performance. For example, it is known in general that missed and extra beats increase with increasing noise interference or that decreasing sensitivity decreases extra beats at the expense of increasing missed beats. However, for a specific S/N (signal to noise ratio), threshold setting, heart signal shape and noise PDS, the expected probability of false and missed beats is not known. This is because it is nearly impossible for a subject to maintain constant repeatable signal conditions for a sufficient time to collect enough data to calculate the probability of missed and extra beats with any statistical

confidence. Measurement of S/N is another problem since the signal and noise are not easily separated. A solution is to simulate heart signal power to noise power conditions that exist for a long enough period of time (up to 1000 beats at a constant heart rate) to establish detection probabilities. Using the signal models described in Chapter II and an appropriate test set up, experimental measurement of detection probability as a function of S/N and threshold is then possible. The results are then presented in the form of ROC (receiver operating characteristic) curves for convenient absolute and relative performance evaluation.

3.2 Experimental Method

In Chapter II, models for simulating ECG, EMG and artifact signals were presented. The combined implementation of the models provides a steady state heart signal in noise, where the relative power of the component signals may be varied. Two reference heart signals each consisting of 1000 continuous noise free beats at 70 BPM and 180 BPM were recorded on a FM (frequency modulated) instrumentation tape recorder with a 300 Hz band width and better than 40 dB S/N. The 180 BPM reference heart signal was empirically simulated from a lower rate heart signal as mentioned in Chapter II. The EMG noise simulation used a low frequency Gaussian noise source filtered as shown in Fig. 3.1. The frequency response of the filter corresponds to the specification of equation 2.2,

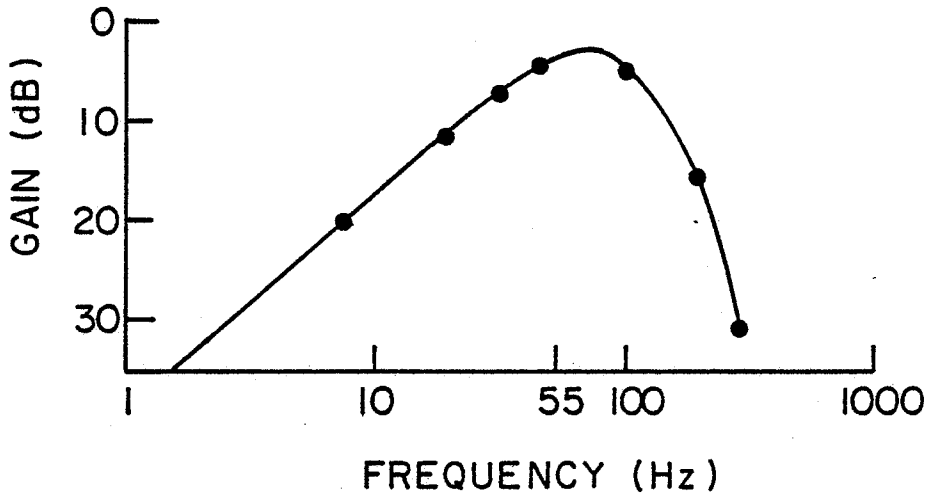

Fig. 3.1 EMG simulation filter response

with additional 24 dB/octave low pass filtering above 100 Hz to reduce the noise power at 230 Hz to 10 dB below the 20 Hz level. This allows a minimum sampling rate of 250 Hz. The EMG noise was recorded on a channel adjacent to the heart signal for simultaneous playback. Artifact noise was simulated by passing 0 Hz to 150 Hz Gaussian pseudorandom noise through a 1 Hz single pole low pass filter. The sequence length was 5.5 minutes (Fig. 3.2).

The three signal components were then added (Fig. 3.2) in various proportions to simulate actual S/N conditions for QRS detector testing. This required the measurement of component signal power levels to determine quantitative values for S/N. Since direct power measurement of low frequency signals is difficult, a calibration procedure was used. The separate ECG and EMG signals were played back 16 times faster than their recorded speed and the power level at the tape recorder output was measured with an AC coupled true RMS voltmeter. A reference oscillator at 100 Hz was then set to the same level measured for ECG and EMG, utilizing a feature of the tape machine that connects the input channels through to the output channels in the stop mode. The ECG and EMG signal levels could then be quickly adjusted with the machine stopped. This technique measured the power of the ECG and EMG signals in a .05 to 300 Hz band. The calibration procedure was verified by checking the nominal 3.75 peak to RMS factor for a Gaussian distribution by observing the expected peak voltage on an oscilloscope. The peak to RMS voltage factors of 8.1 and

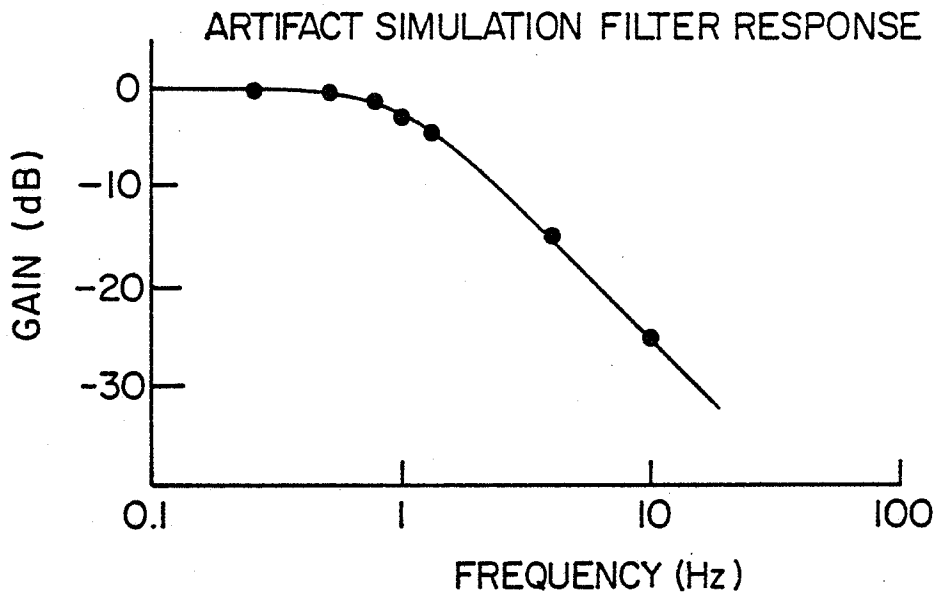

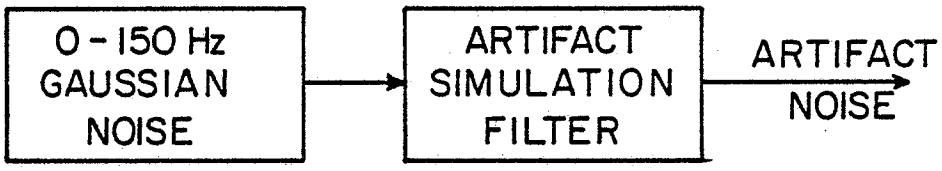

Fig. 3.2 Artifact noise simulation

5.8 for the 70 BPM and 180 BPM reference heart signals respectively were within the full scale maximum crest factor of 10 required to maintain the accuracy of the true RMS voltmeter. The calibration procedure was used consistently for all ECG and EMG signal level measurements. Fig. 3.3 shows the equipment configuration.

Artifact noise being very low frequency could not be measured in the same manner as ECG and EMG signals. Instead the PDS calibration feature of the low frequency Gaussian noise generator was used [13], corrected by the power gain of the low pass filter. The calibration was verified by observing the expected peak level. Since the instrument synthesizes Gaussian noise digitally, the calibration technique is analytically determined and is inherently stable. The digital nature of the noise generator also ensures that the output signal has a Gaussian amplitude distribution with known error limits.

The S/N ratio referred to in testing was defined as the ratio of heart signal power over the total noise power expressed in dB,

$$S/N = 10 \log_{10} \left[\frac{\frac{1}{T} \int_0^T s^2(t) \, dt}{\frac{1}{T} \int_0^T n^2(t) \, dt} \right] \text{ dB} \qquad (3.1)$$

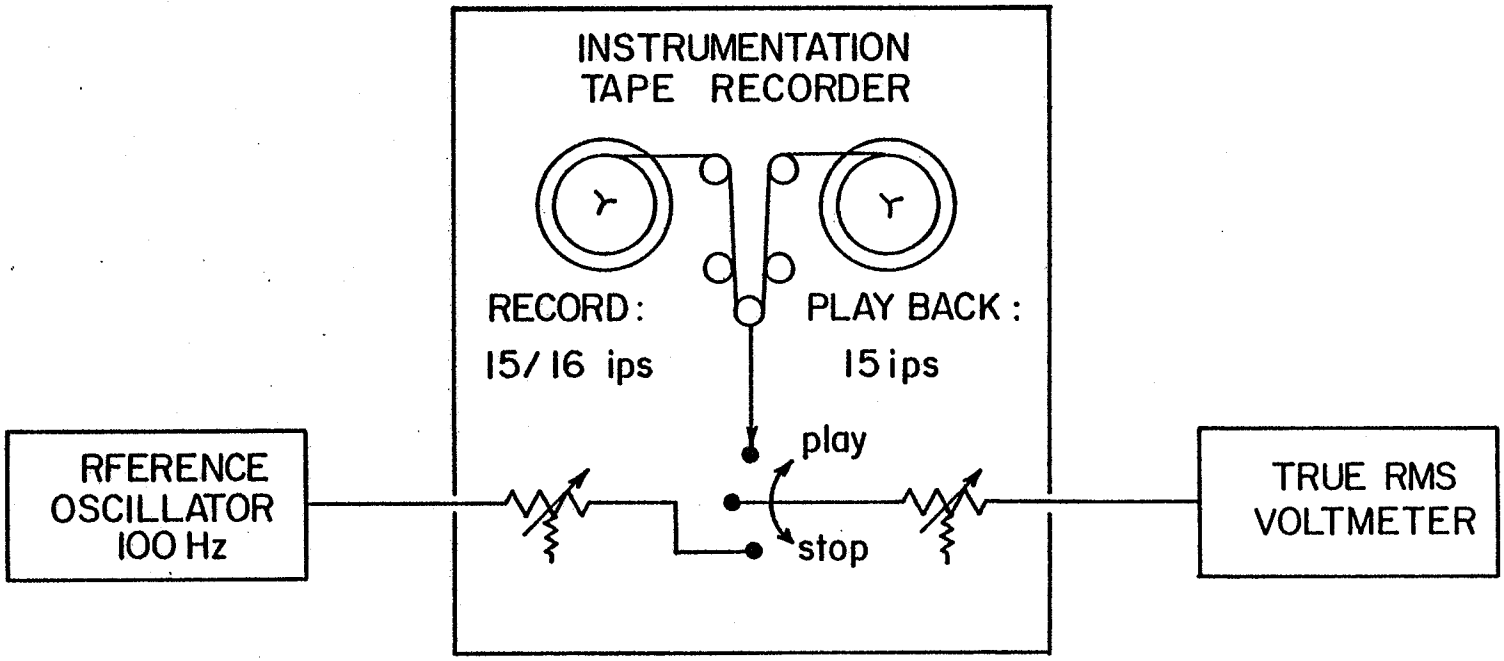

Fig. 3.3 Recorded ECG and EMG signal power measurement

The total noise term is the sum of EMG and artifact noise. Varying the proportions of EMG and artifact noise effectively changes the PDS of the total noise (review Fig. 2.7). The standard proportion of noise chosen was EMG noise power equal to artifact noise power. This ratio was determined by observing very noisy ECG records and estimating the worst peak EMG and artifact noise voltages. For a 1 V p-p heart signal, the EMG and artifact noise were about 1 V p-p each. The worst case signal to EMG noise ratio was evaluated by a simple experiment. Electrodes were placed on a subject's wrists (reference lead placed on the abdomen). The noisy signal resulting from one minute of isometric exercise of the biceps lifting an immovable bench was recorded. The heart signal was then recorded for one minute. Since the noise was predominately EMG noise, the total noise plus signal power followed by the signal only power were measured by the fast playback procedure. The S/N was calculated to be about -6 dB. Adding equal artifact noise as noted previously and considering that the wrists are susceptible electrode locations for ECG noise interference, a -6 to -9 dB total signal to noise ratio is about the worst that may be expected. Simulated equal EMG and artifact noise interfering with the 180 BPM reference heart signal are shown in Fig. 3.4.

The -6 to -9 dB S/N range is considered the lower limit to specify desired QRS detection in terms of minimizing P_F (probability of false detection) and maximizing

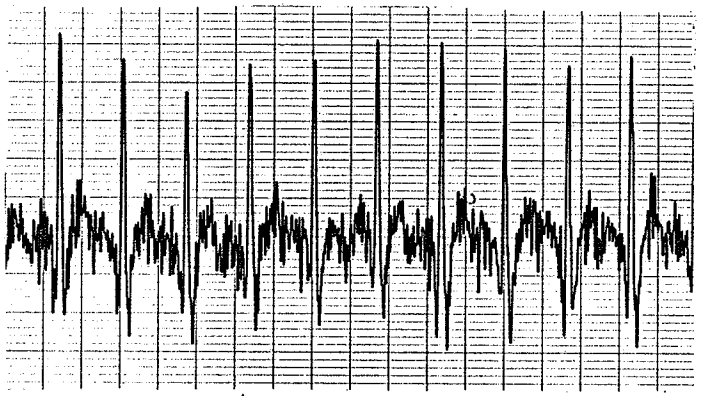

(a) +7.0 dB

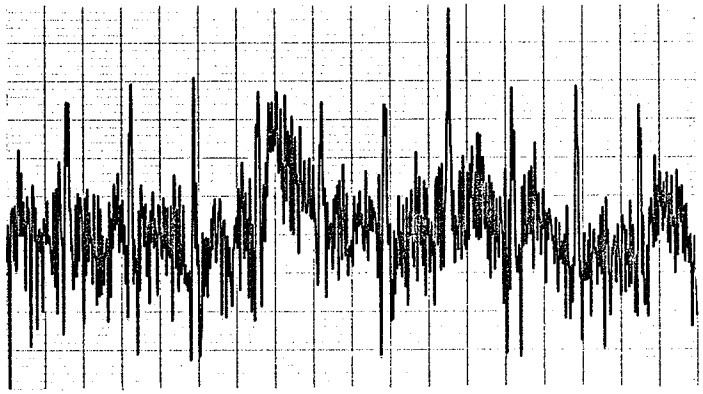

(b) -3.0 dB

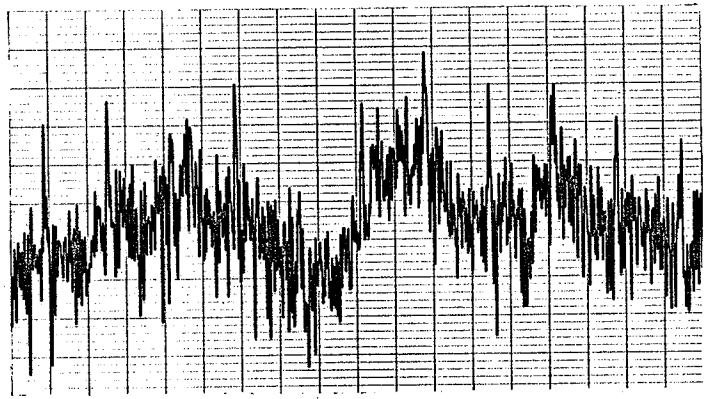

(c) -6.0 dB

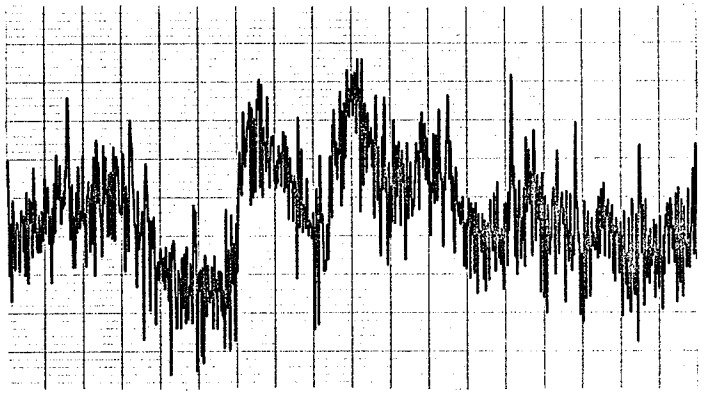

(d) -9.0 dB

Fig. 3.4 180 BPM reference signal plus equal power artifact and EMG noise at various S/N.

P_D (probability of detection). A typical design specification might require a less than 2% total error rate with a S/N of -6 dB. Such a specification implies that P_F and P_D must be measured.

The measurement of P_F (probability of false detection) and P_D (probability of detection) in QRS detection was accomplished with a coincidence detector as shown in Fig. 3.5. The circuit determined the occurrence of the reference heart beat before attenuation and noise corruption using a standard bandpass threshold QRS detector. From the reference detector a nominal 50 mS time window was established during which the QRS detector being evaluated should also indicate a beat. If the beat occurred, a coincidence beat (B_c) counter was incremented, and subsequent test beat indications were locked out until the next open time window. The total reference beats (B_r) and the total test beats (B_t) were counted. P_D and P_F were then defined as:

$$P_D = \frac{B_c}{B_r} \triangleq \frac{\text{coincident received beats}}{\text{total beats sent}} \qquad (3.2)$$

$$P_F = \frac{B_t - B_c}{B_t} \triangleq \frac{\text{noncoincident beats received}}{\text{total beats received}} \qquad (3.3)$$

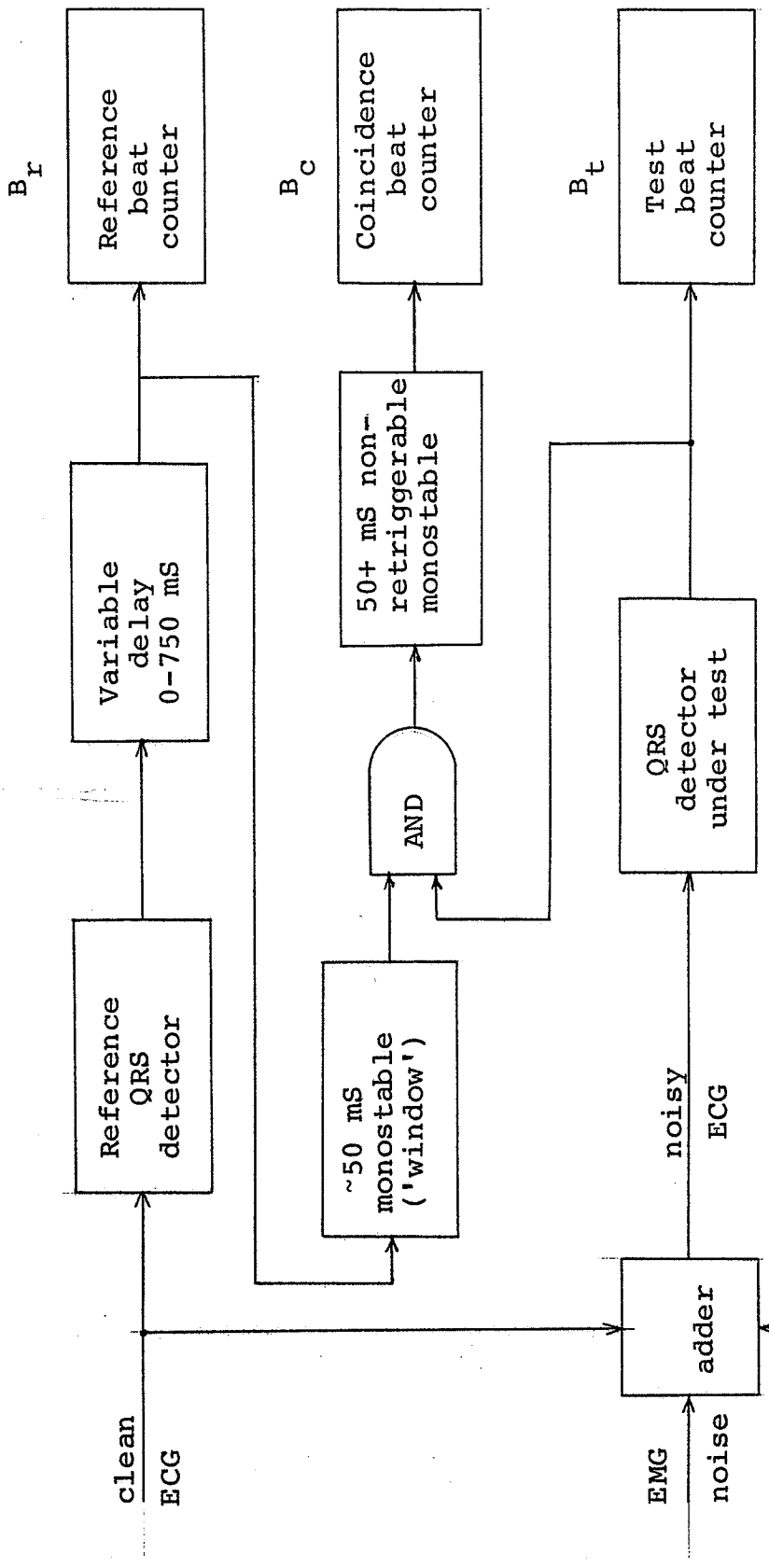

Fig. 3.5 Measurement of QRS detector performance.

For the given S/N applied to the QRS detector under test, the P_D and P_F parameters may be determined for all reasonable sensitivity settings. As the measurement is statistical in nature, longer trials produce more confident results. It was found that 1000 beats yielded repeatable results for the range of P_D and P_F measured (0.005 to 0.5 and 0.5 to .995 respectively). The EMG noise was recorded coincident with the heart signal and the artifact noise generator sequence was always reset at test commencement, therefore, any weighting due to a limited sample size is the same for all tests.

It was found that 12 to 20 ECG record replays of 300 to 1000 beats with noise were required to characterize a QRS detector over the appropriate range of S/N and threshold settings. The time required per characterization was about 2 hours. This did not include the time required for the assembly, calibration and verification of the test set up.

3.3 Receiver Operating Characteristics

The experimental method of QRS detector evaluation appears to involve the collection of a large amount of data. Each of the 12 to 20 combinations of the variables S/N and threshold required to characterize a QRS detector generate a corresponding set of P_D and P_F values. In order to present the data in a meaningful manner, the concept of an ROC (Receiver Operating Characteristic) curve from communication theory was used. A good explanation of ROC curves and their properties is offered in [11]. In this application as shown in Fig. 3.6, lines of constant S/N are used while the sensitivity of T (threshold) is varied to move along a line of constant S/N. Increasing T moves the operating point along the curve to the lower left hand corner where $P_D = 0$ and $P_F = 0$. Decreasing T moves the operating point along the curve to the upper right hand corner where $P_D = 1$ and $P_F = 1$. Clearly, there is a threshold that minimizes the sum of P_M (probability of a missed beat, where $P_M = 1 - P_D$) and P_F. The point on the constant S/N curve that is closest to the upper left hand corner where $P_D = 1$ and $P_F = 0$ minimizes total error [11]. The ideal QRS detector would operate in the $P_D = 1$, $P_F = 0$ corner for every S/N ratio.

Signal detection theory establishes the existence of a bound on the highest performance attainable in coloured Gaussian noise as a function of S/N and signal shape. The matched filter including prewhitening should determine

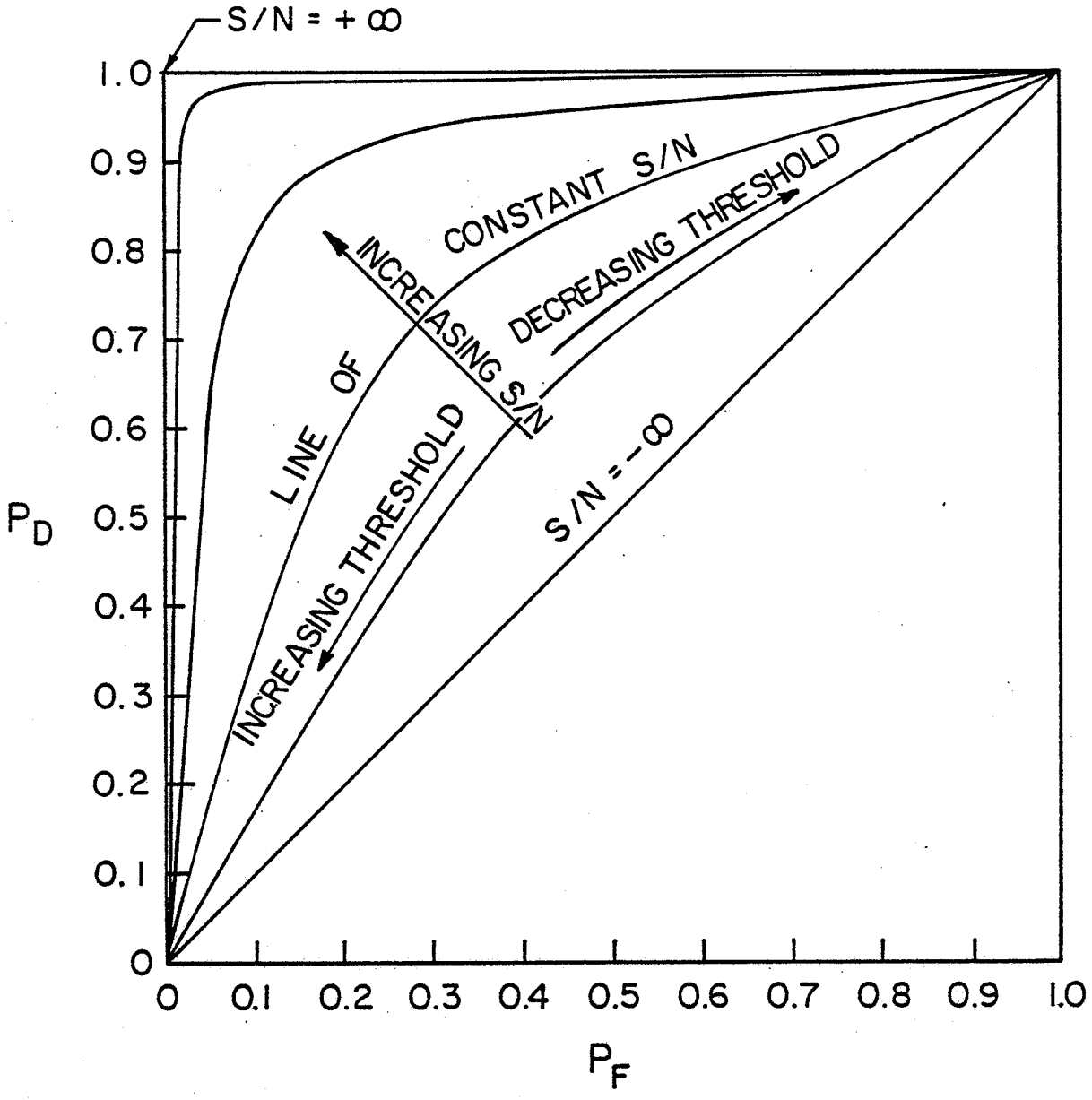

Fig. 3.6 Example ROC curve

bound and should determine how closely other QRS detector schemes approach it. Two QRS detectors tested with the same signals are compared by determining the lines of constant S/N that are closest to the ideal operating point. The difference in S/N for the same performance can be used as a measure of performance. For example, indicating QRS detector 'A' is 3 dB better than QRS detector 'B' means that device 'A' can tolerate 3 dB (1.41 voltage factor) more noise for the same performance as device 'B' for any given threshold. The ROC also provides information for limiting P_F for given S/N condition. In signal averaging, P_F can be limited at the expense of P_D. This amounts to weighting P_F and P_D in the performance criteria for the particular application. Turin [3] points out a parallel example of a typical radar detection problem where P_F is set to the maximum tolerable level. The resulting P_D for a given S/N defines the measure of performance. Aside from performance evaluation, ROC curves were used in this thesis to quantitatively investigate sensitivity of the matched filter detector to heart signal shape variation and to noise PDS variation.

3.4 Test Configuration

Components of the test configuration have been referred to previously in a general manner. The complete block diagram is presented in Fig. 3.7. The specific details of commercial and developed instrumentation used can be found

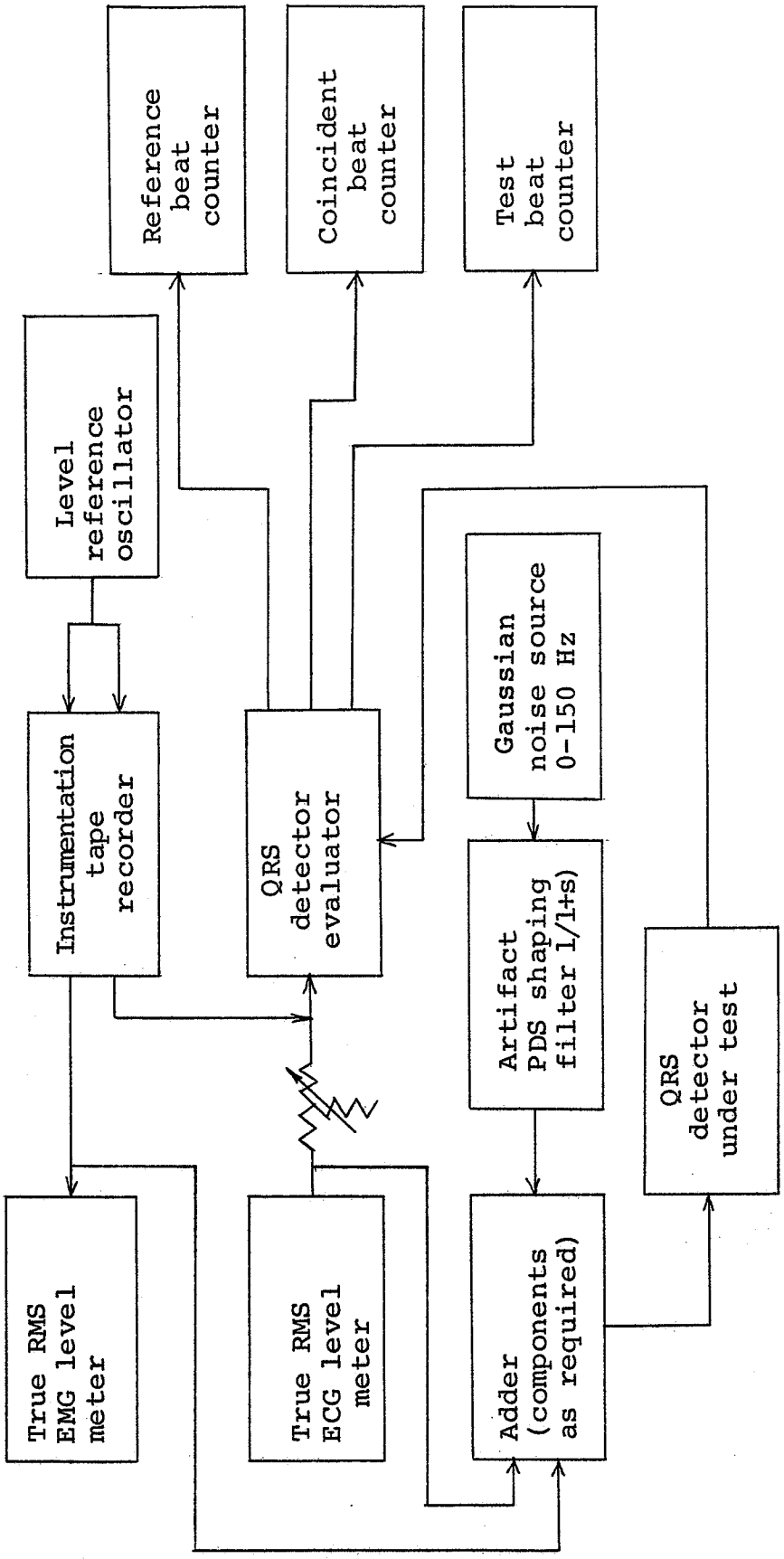

Fig. 3.7 QRS detector testing configuration

in Appendix B. Hopefully, the background information of the previous chapters and the appendix make Fig. 3.7 self-explanatory. What remains to be clarified is the design philosophy of the test set up and procedure.

QRS detector evaluation by generating ROC curves required the interconnection of about 15 pieces of test equipment. Therefore, ease of operation was an important consideration. Wherever possible, instrument interconnections were made with BNC connectors for reliability and simplicity. Principles of instrumentation /14/ were observed to eliminate extraneous noise due to ground loops and the like. Impedance coordination between instruments was considered to prevent signal level discrepancies due to loading or mismatch. The frequency response of signal paths were verified and AC coupling was used carefully when required due to the low frequency nature of the signals involved. Correct operation of the system was established at a subsystem level before overall verification of system function. Gains and levels were monitored before and during testing. Operating points on the ROC curves were periodically checked for repeatability. Development of a realiable test configuration and procedure was emphasized. This was due to the statistical nature of the tests, where errors in set up and procedure are hard to detect. Statistical testing is time consuming, therefore, repeating tests due to errors needlessly slows progress. Despite all precaution, inevitable mistakes were made and subsequently corrected. However, the test method was never

the focus of concern as it produced confident and consistent results throughout.

3.5 Matched Filter QRS Detector Realization

The matched filter QRS detector was realized on a digital computer in real time. Fig. 2.10 indicates the canonical form of the transversal filter used. This form was preferred as it could be implemented with fewer programmed steps compared to the hardware oriented delay line approach. The transversal filter used 8 bit weights that were loaded from a data file containing the filter specification h(t), created by the immediate mode digital signal processing procedure shown in Fig. 2.9. The final sampling frequency was 250 Hz. The maximum number of weights or taps possible at this sampling rate was 100, limited by multiplication time. The incoming analogue signal was converted to an 8 bit 2's complement digital value. Two outputs were available from the detector. One was the resultant analogue signal converted from a 12 bit digital value before threshold comparison. The other was the 5 V, 5 mS pulsed output of the digital threshold comparator. The threshold could be set and monitored during program execution, using a potentiometer and digital readout available on the front panel of the data acquisition system associated with the computer. The program had a run mode and threshold set mode controlled by a computer console switch.

The program was written in assembly language. For real time operations, assembly language offers the greatest potential for maximizing execution speed. Since the program

had to be fast, it was short. The current version is 870 16 bit words long, of which 40 words are required for transversal filter instructions and 50 words are required for comparison operations. The balance of the program is support software and scratchpad memory.

The program was created for development purposes only. It is not professionally written with extensive documentation and appropriate routines to handle anticipated user or system errors. This is justifiable as it is unlikely a 16 bit minicomputer would be used for stand alone QRS detection. A simpler machine would suffice.

The program's operation was verified by comparing its finite impulse response with the particular h(t) specified. Care was taken to minimize truncation and round off error. An ROC curve was generated using 4 bit weights and compared to the 8 bit results to verify that quantization noise and finite word length arithmetic were not significant enough to affect performance. There was no discernable difference between 4 bit and 8 bit results.

Practical 8 bit microprocessor implementation was kept in mind during program development. Eight bit data lengths and 8 bit byte oriented operations were used throughout. Appendix C contains the program source listing with supporting documentation. Fig 3.8 summarizes minicomputer matched filter QRS detector implementation.

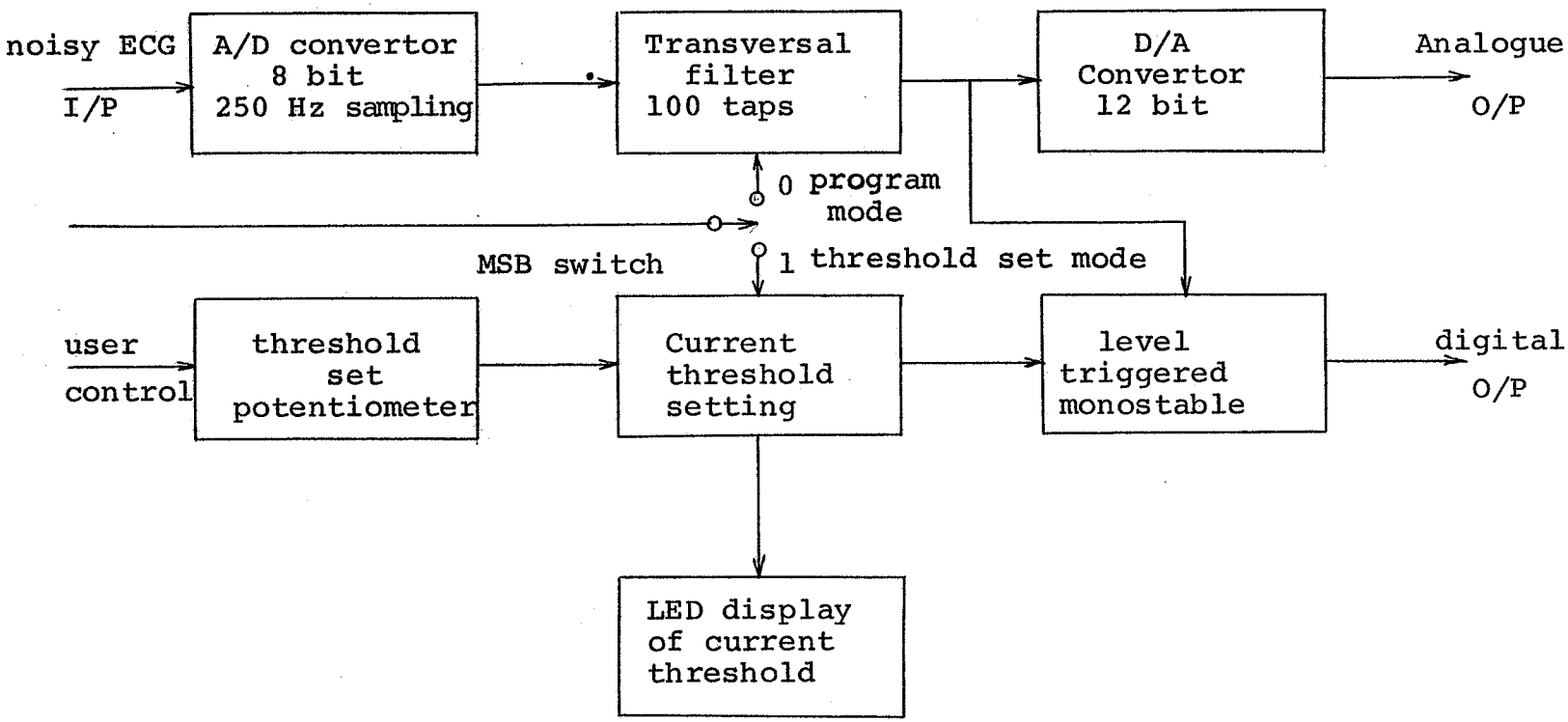

Fig. 3.8 Computer implementation of matched filter QRS detector.

CHAPTER IV

TEST RESULTS

4.1 Introduction

The QRS detector evaluation tests fall into two categories, comparison of the matched filter QRS detector with other QRS detectors and the investigation of matched filter sensitivity. The matched filter QRS detector ROC curve by itself has little meaning without comparable curves from other detectors. The sensitivity tests provide an insight into the matched filter's tolerance to mismatch. If the performance of the matched filter detector warrants implementation in real systems, sensitivity tests may furnish needed design information.

Two QRS detectors other than the matched filter were tested. One was a commercial unit presently in use at the Health Sciences Centre, Winnipeg, Manitoba. The other was a prototype model available at the St. Boniface Hospital, Winnipeg, Manitoba based on the design of Winter and Trenholm [2]. The five heart signals used for sensitivity testing were recorded from volunteer subjects from the student body at this university. The Winter-Trenholm QRS detector was considered the best available at present, thus providing a good basis for comparison. The reference 70 BPM heart signal had a very high T wave, a known problem signal for existing detectors. Other heart signals were chosen for their deviance from the reference 180 BPM signal. The strategy was to benchmark the performance of the matched filter QRS detector.

4.2 QRS Detector Performance Comparison

Block diagrams of the two QRS detectors used for performance comparison with the matched filter QRS detector are shown in Fig. 4.1. The unit from the HSC (Health Sciences Centre) is a conventional band pass filter, threshold detecting device with a 235 mS refractory period and a simple AGC (automatic gain control). The Winter-Trenholm prototype determines the zero crossings of the noisy signal. A QRS occurrence is indicated when a positive zero crossing is followed by a negative zero crossing within a specified minimum and maximum time. This is a form of wave period processing.

The threshold level of the HSC QRS detector was fixed, so threshold variation was accomplished by changing the absolute value of the signal and noise by the same amount. The Winter-Trenholm detector threshold variation was facilitated by an input amplifier gain control. The minimum and maximum time windows on the Winter-Trenholm unit were set with no noise added according to the guidelines of [27]. The minimum time setting for the 70 BPM reference heart signal was 16 mS and the maximum time setting was 28 mS establishing a 12 mS window with a detected QRS wave centered at 22 mS. The same method was used to establish a centered 12 mS window for the 180 BPM reference signal.

St. Boniface Hospital prototype QRS detector
(Winter-Trenholm type)

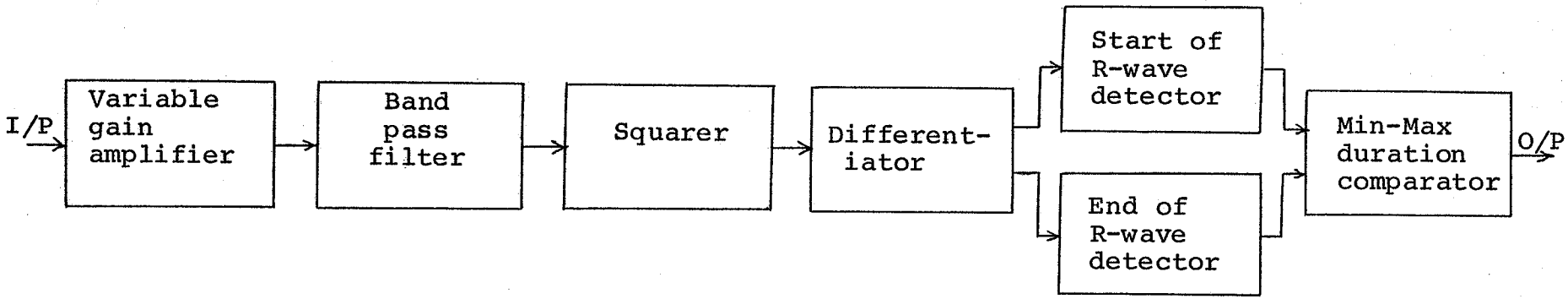

Health Sciences Centre QRS detector

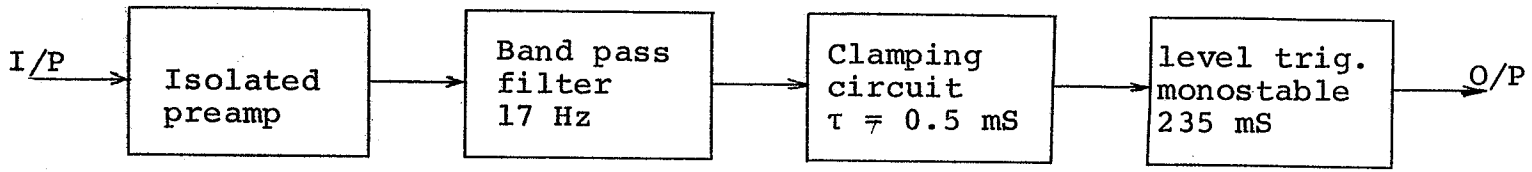

Fig. 4.1 Performance comparison QRS detectors

Three series of comparison tests were performed on the HCS, Winter-Trenholm and matched filter QRS detectors. Series one and two measured the performance of all the detectors with EMG noise interference only at 70 BPM and 180 BPM respectively. The third series established performance of the Winter-Trenholm and matched filter detectors at 180 BPM with equal power interfering EMG and artifact noise. In the first two series, the matched filter h(t) was prewhitened for a 1:4 (Artifact:EMG) power ratio even though the interfering noise was EMG only. In initial attempts to use a finite time h(t) prewhitened to EMG noise only, the heart signal could be detected with no missed or extra beats at a -19.0 dB S/N (Fig. 4.2). This was due to the very high relative dc gain of the EMG only h(t). Meaningful ROC curves could not be generated for this filter, as dc drift at the mV level in the set up become a significant source of noise. It was concluded even minimal artifact noise would make the finite time EMG only matched filter detector impractical. High heart rates would also cause severe aliasing at the filter output preventing meaningful QRS detection. The matched filter h(t) used for the third series of comparison tests was prewhitened for equal power EMG and artifact noise.

Table 4.1 summarizes the resulting ROC curves (Fig. 4.3) of the first test series at 70 BPM.

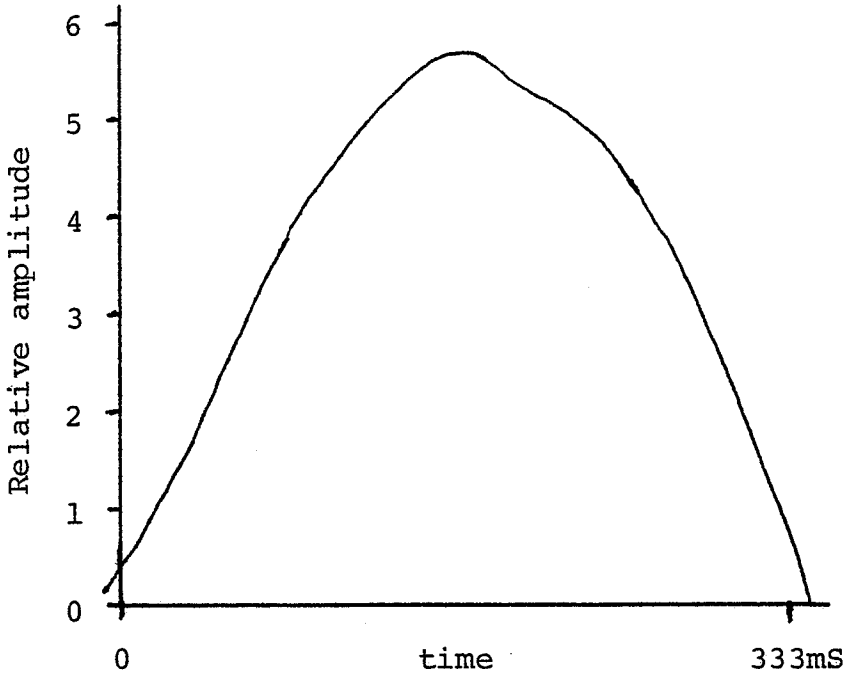

(a) Finite time interval h(t) for EMG noise only

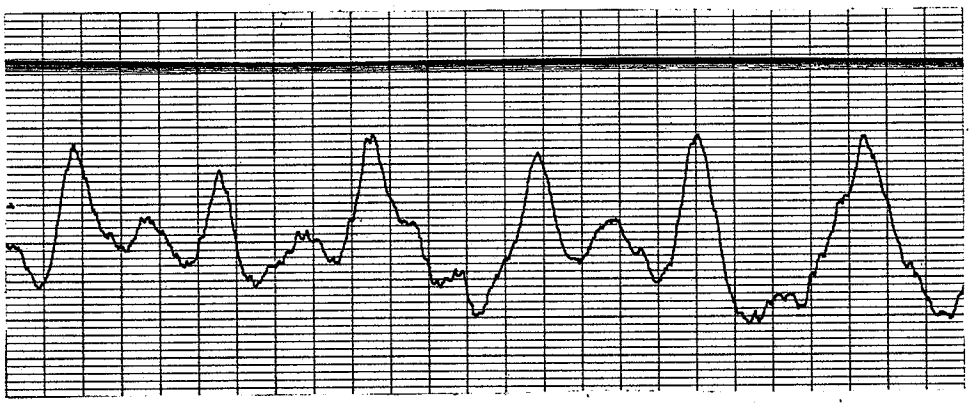

(b) Output of h(t) with an input of -27.0 dB. S/N 70 BPM reference heart signal and EMG noise.

Fig. 4.2 Finite time interval h(t) and response to noisy low rate heart signal.

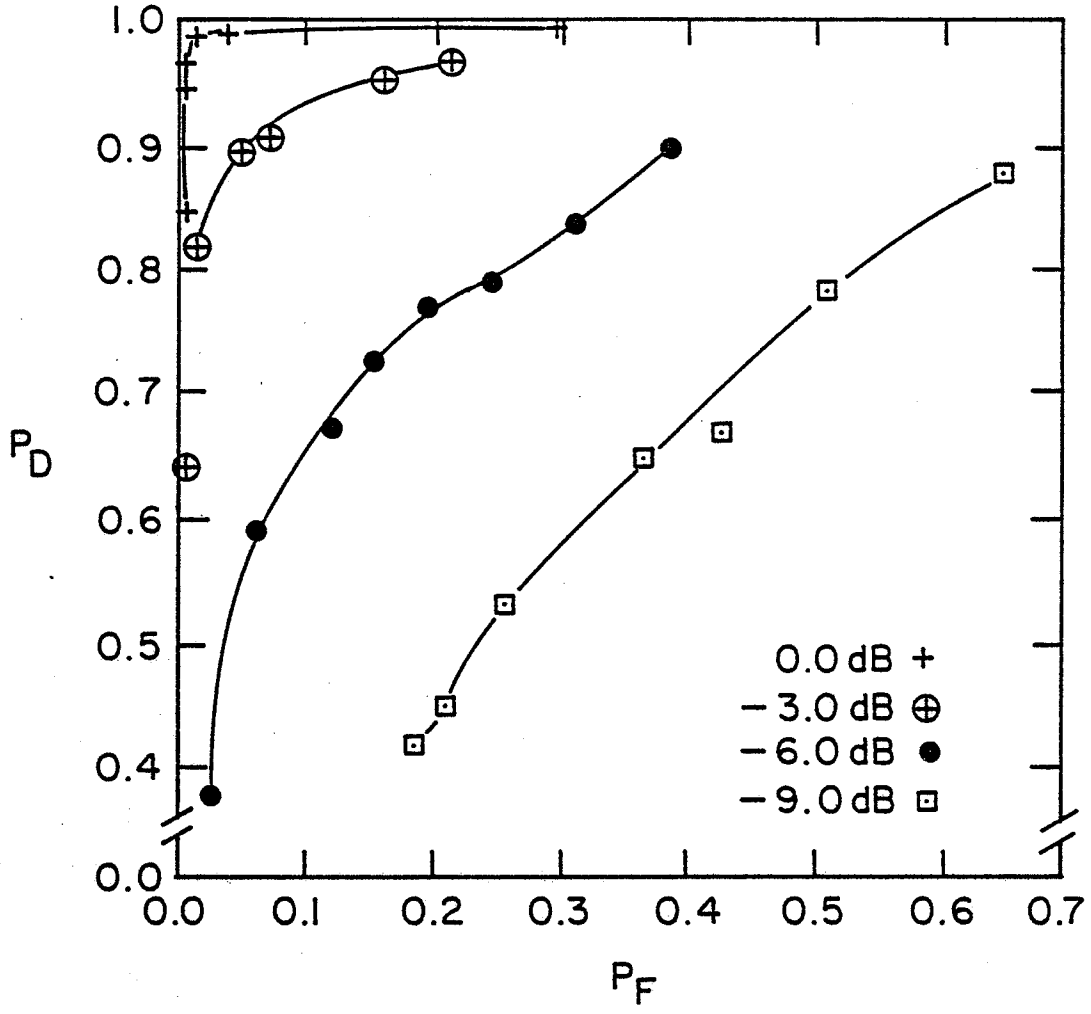

QRS detector: Winter-Trenholm prototype

Heart signal: 70 BPM reference

Noise: EMG only

Fig. 4.3(a) Series 1 comparison ROC curves

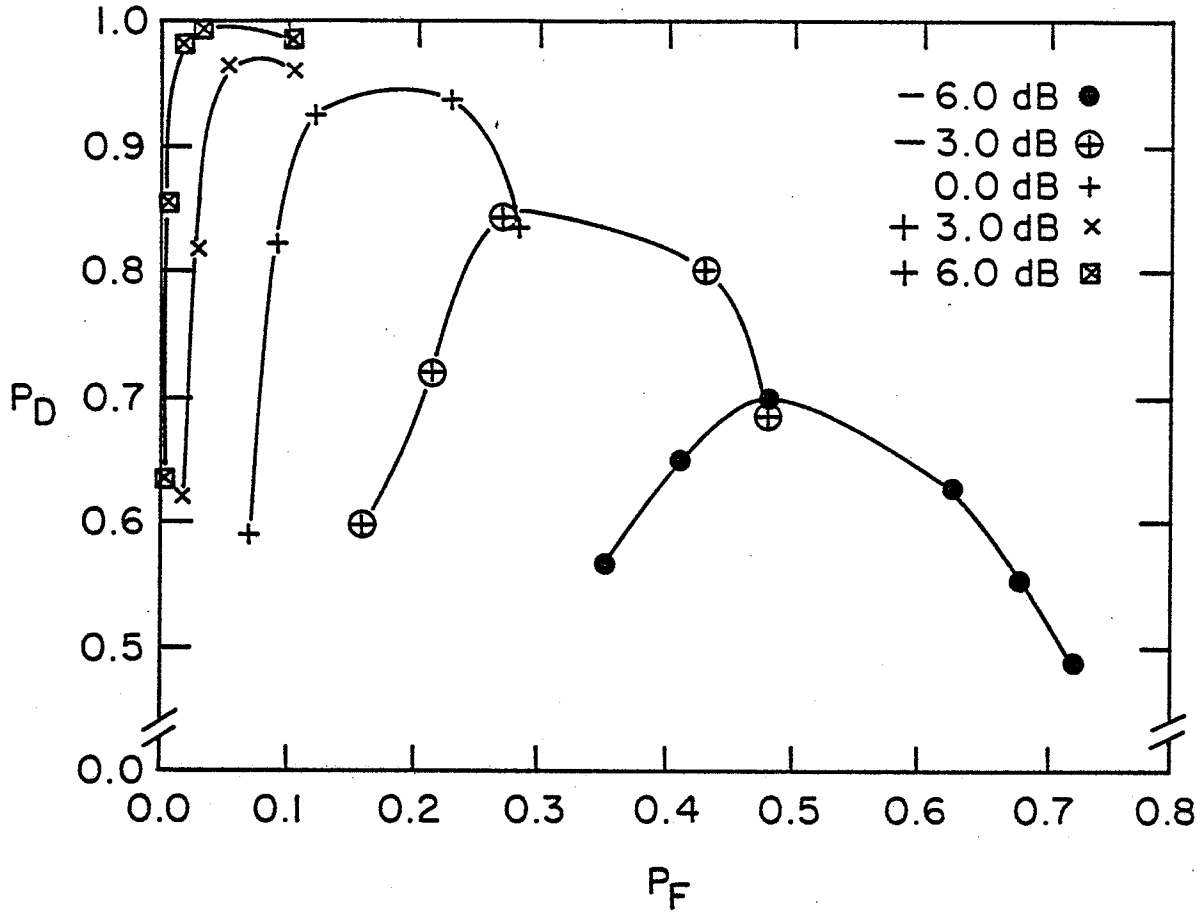

QRS detector: HSC commercial unit

Heart signal: 70 BPM reference

Noise: EMG only

Fig. 4.3(b) Series 1 comparison ROC curves

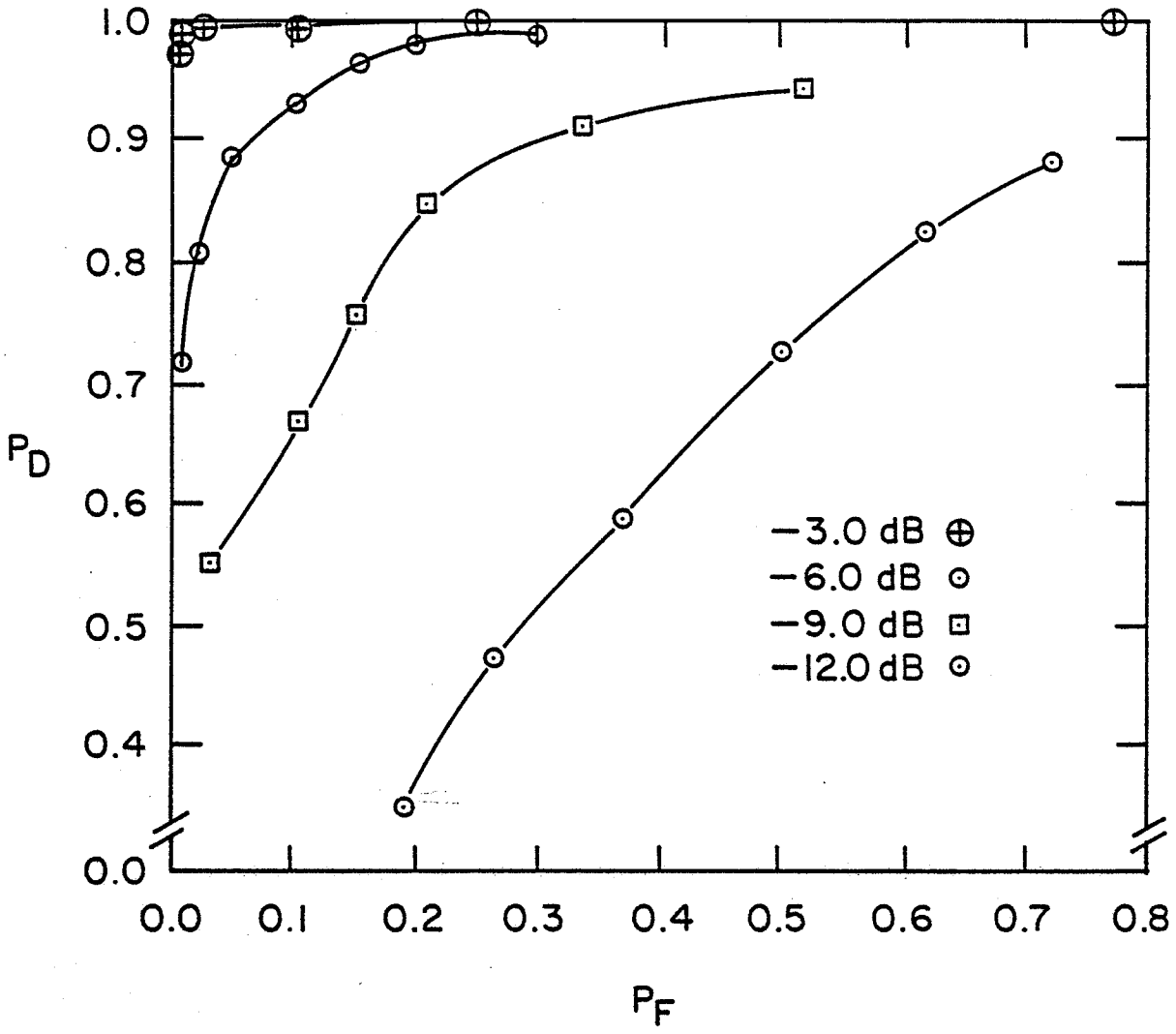

QRS detector: Matched filter (h(t) prewhitened for a 1:4 Artifact to EMG power ratio)

Heart signal: 70 BPM reference

Noise: EMG only

Fig. 4.3(c) Series 1 comparison ROC curves

QRS Detector	Operating Point P_D	P_F	S/N (dB)
Matched Filter	0.92	0.08	-6.0
Winter-Trenholm	0.91	0.07	-3.0
Commercial	0.92	0.12	-0.0

Table 4.1

Summary of QRS detector performance with 70 BPM reference signal plus EMG noise.

Note the HSC detector ROC curve contained in Fig. 4.3 exhibits a reduced P_D after a certain decrease in threshold. This is due to the 235 mS refractory period after detection which is intended to suppress false triggering on high T waves. In heavy noise situations false triggering tends to lock out true QRS triggering, causing P_D to decrease. Normally, increased sensitivity increases P_D.

Table 4.2 summarizes the 180 BPM series EMG noise only ROC curve test results contained in Fig. 4.4.

QRS Detector	Operating Point P_D	P_F	S/N (dB)
Matched Filter	0.93	0.08	-12.0
Winter-Trenholm	0.94	0.07	- 9.0
Commercial	0.91	0.08	- 6.0

Table 4.2

Summary of Detector Performance with 180 BPM reference signal plus EMG noise.

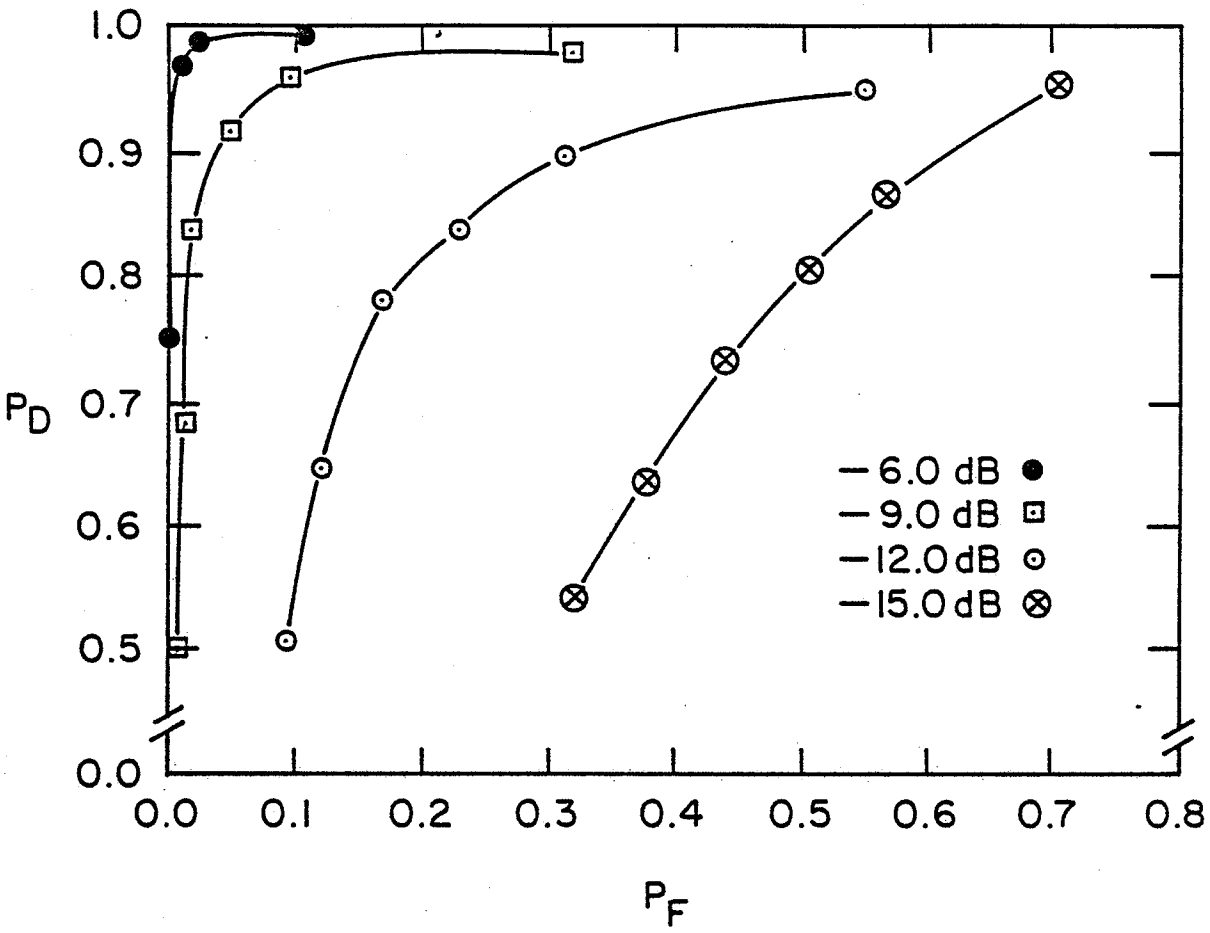

QRS detector: Winter-Trenholm prototype

Heart signal: 180 BPM reference

Noise: EMG only

Fig. 4.4(a) Series 2 comparison ROC curves

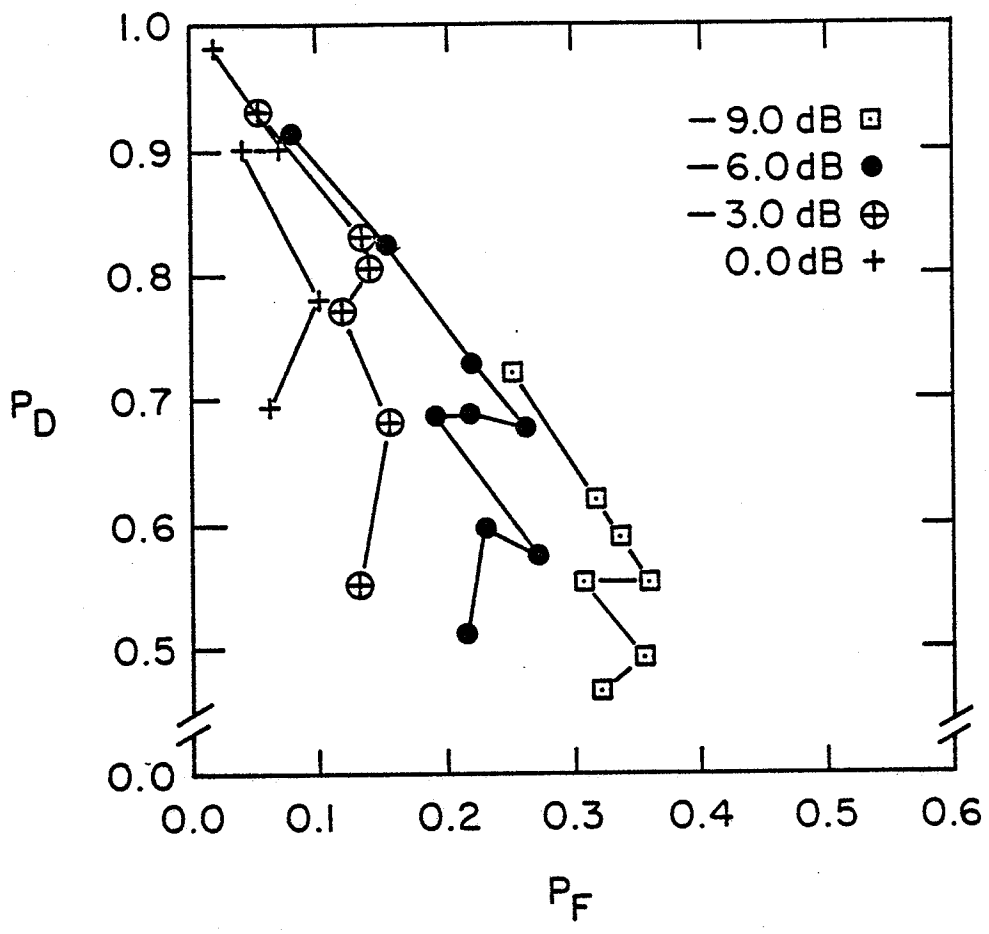

QRS detector: HSC commercial unit

Heart signal: 180 BPM reference

Noise: EMG only

Fig. 4.4(b) Series 2 comparison ROC curves

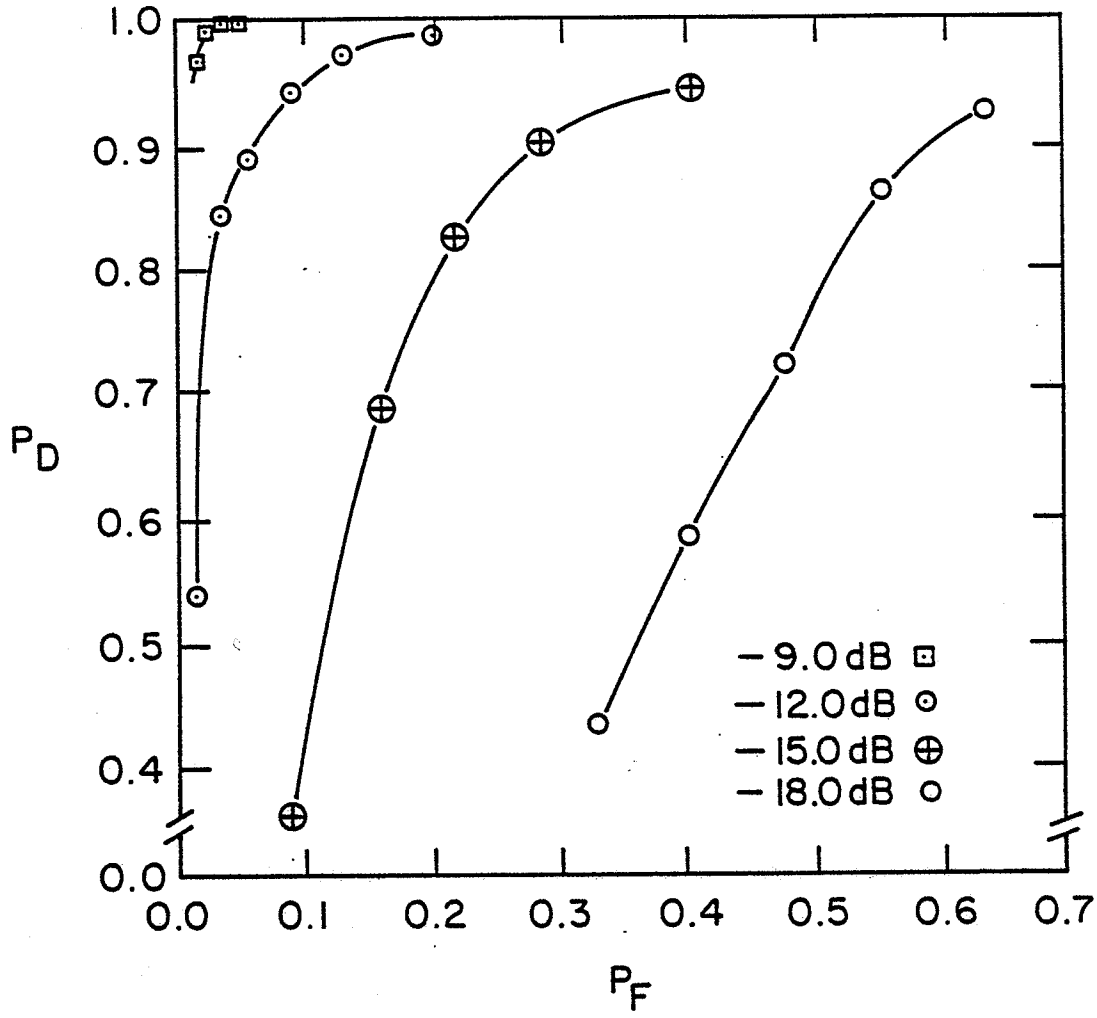

QRS detector: Matched filter (h(t) prewhitened for a 1:4, Artifact to EMG power ratio)

Heart signal: 180 BPM reference

Noise: EMG only

Fig. 4.4(c) Series 2 comparison ROC curves

The ROC results for the HSC detector are difficult to interpret. It was determined that the unit uses an AGC circuit equivalent to a capacitor and diode clamp at the comparator input. The time constant was such that the 180 beat signal greatly enhanced the AGC effect. To find the peak performance operating point, the absolute level of the signal plus noise was raised until the end point was found.

Table 4.3 summarizes the third series of comparison tests using the 180 BPM reference heart signal and equal power EMG and artifact interference. Fig. 4.5 contains the ROC curve results.

QRS Detector	Operating Point P_D	P_F	S/N (dB)
Matched Filter	0.95	0.05	-9.0
Winter-Trenholm	0.95	0.05	-3.0

Table 4.3

180 BPM, plus equal EMG and Artifact noise performance summary.

The series one tests at 70 BPM with EMG noise only, indicate the matched filter QRS detector tolerates twice the noise power the Winter-Trenholm unit will tolerate for the same performance and tolerates four times the noise power the HSC unit will tolerate for the same performance. The series two tests at 180 BPM with EMG noise only again indicate the matched filter QRS detector tolerates two and four times respectively the noise that the Winter-Trenholm

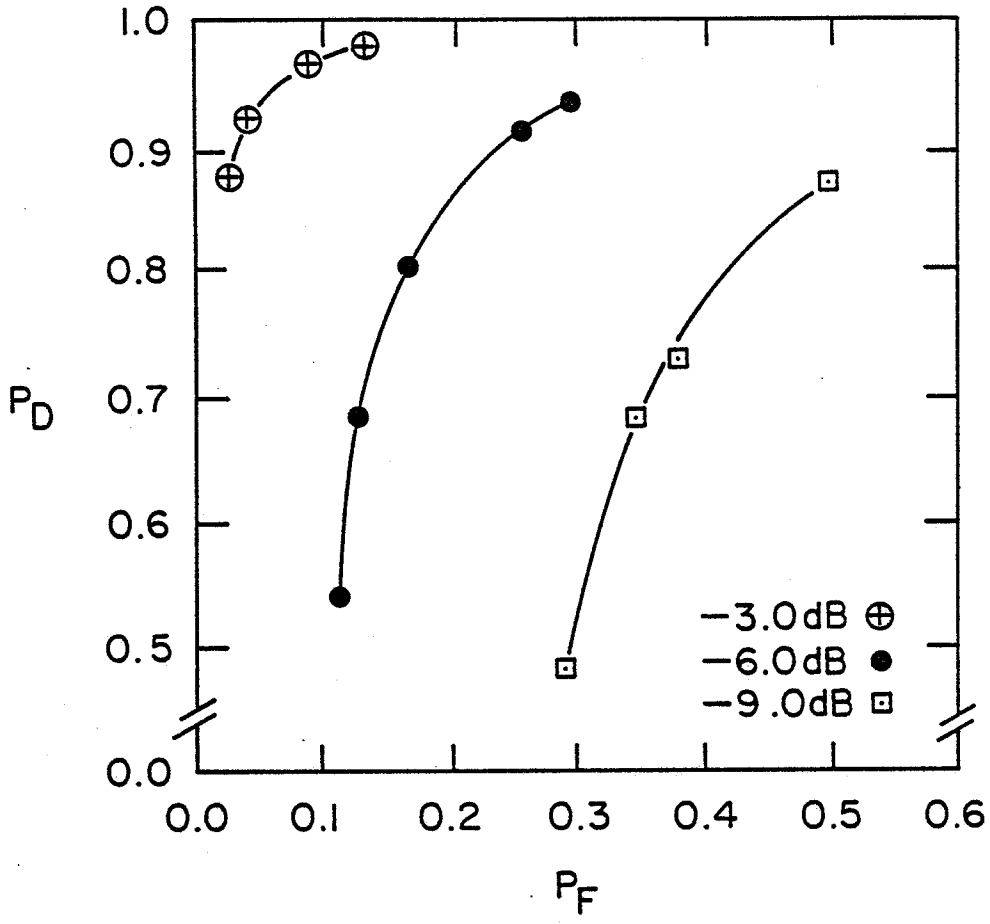

QRS detector: Winter-Trenholm prototype

Heart signal: 180 BPM reference

Noise: 1:1, Artifact to EMG power

Fig. 4.5(a) Series 3 comparison ROC curves

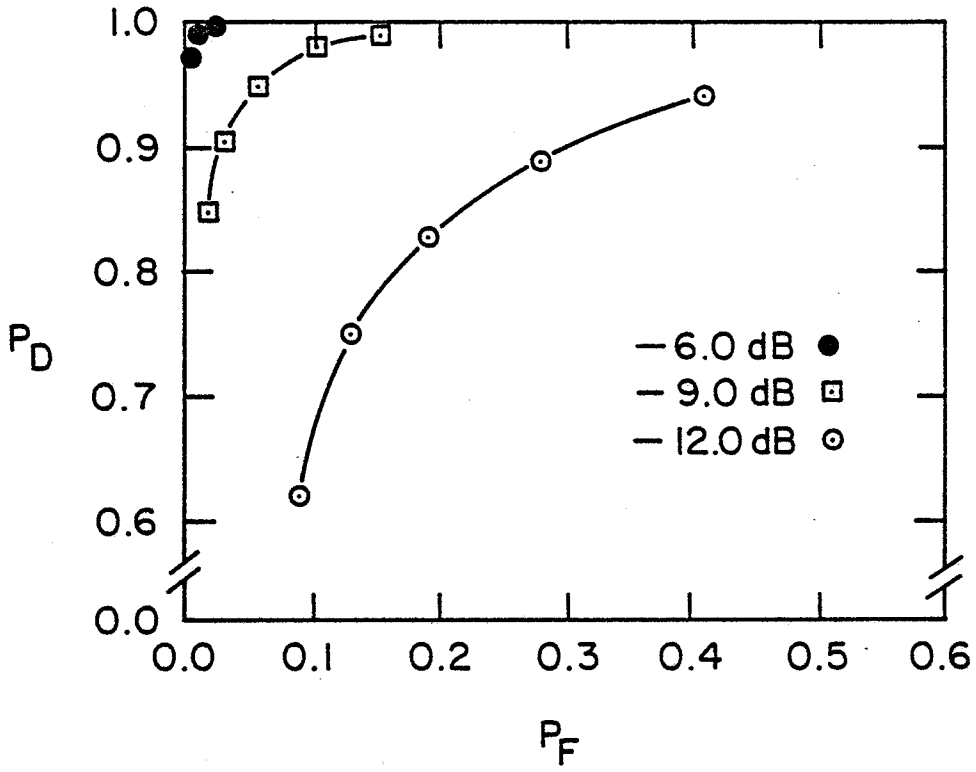

QRS detector: Matched filter (h(t) prewhitened for a 1:1 Artifact to EMG power ratio)

Heart signal: 180 BPM reference

Noise: 1:1, Artifact to EMG power

Fig. 4.5(b) Series 3 comparison ROC curves

and HSC detectors will tolerate for the same performance. The third series of comparison is considered to be closest to a worst case real life situation using equal power artifact and EMG noise to interfere with the 180 BPM reference signal. Here the matched filter tolerates four times the noise the Winter-Trenholm detector will tolerate for the same performance. Under these controlled conditions, the matched filter QRS detector exhibits the best performance in all three test series.

4.3 Performance Sensitivity to Noise PDS

Since the matched filter QRS detector's performance appears attractive from the previous test results, the remaining investigation of its robustness in mismatched situations is a worthwhile pursuit. The optimum h(t) is determined by both s(t) and the noise PDS. In practice, s(t) and the noise PDS are not known exactly. An h(t) may then be mismatched to either signal. Noise PDS mismatch is considered first.

The noise PDS was varied by keeping the individual PDS of EMG and artifact noise constant, while combining them in different ratios. The power ratios used were 16:1, 4:1, 1:1, 1:4, and 1:16 (artifact:EMG). An ROC curve was generated for the 4 new ratios using an h(t) matched to both the 180 BPM reference signal and the particular noise PDS. This determined the upper performance bound for matching to the 180 BPM reference signal and a range of noise PDS. The lower performance bound was derived from the 1:1 noise ratio matched filter ROC curve by realizing that EMG only or artifact only performance cannot be worse than the performance for combined noise. Fig. 4.6 graphically depicts a bounded region of performance for a matched filter prewhitened for equal artifact and muscle noise operating with other noise PDS. Fig. 4.7 contains the four additional ROC curves required to develop Fig. 4.6.

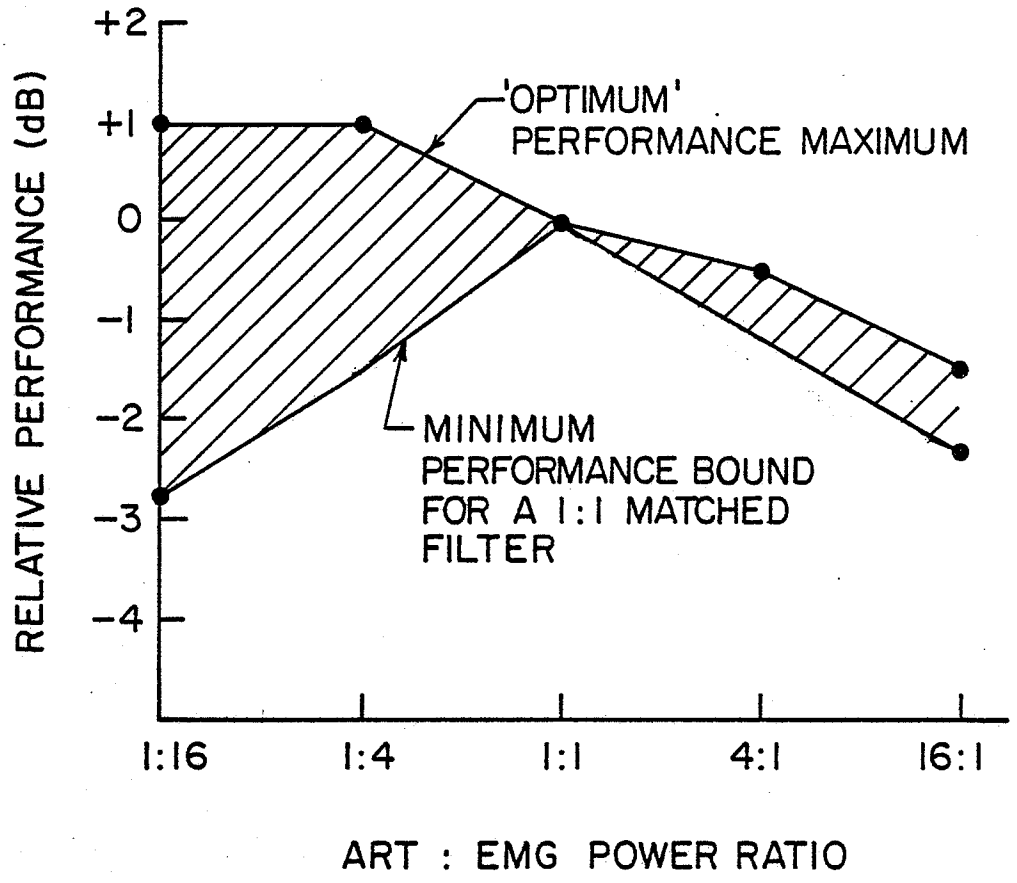

Fig. 4.6 Minimum - maximum performance bounds for noise PDS variation

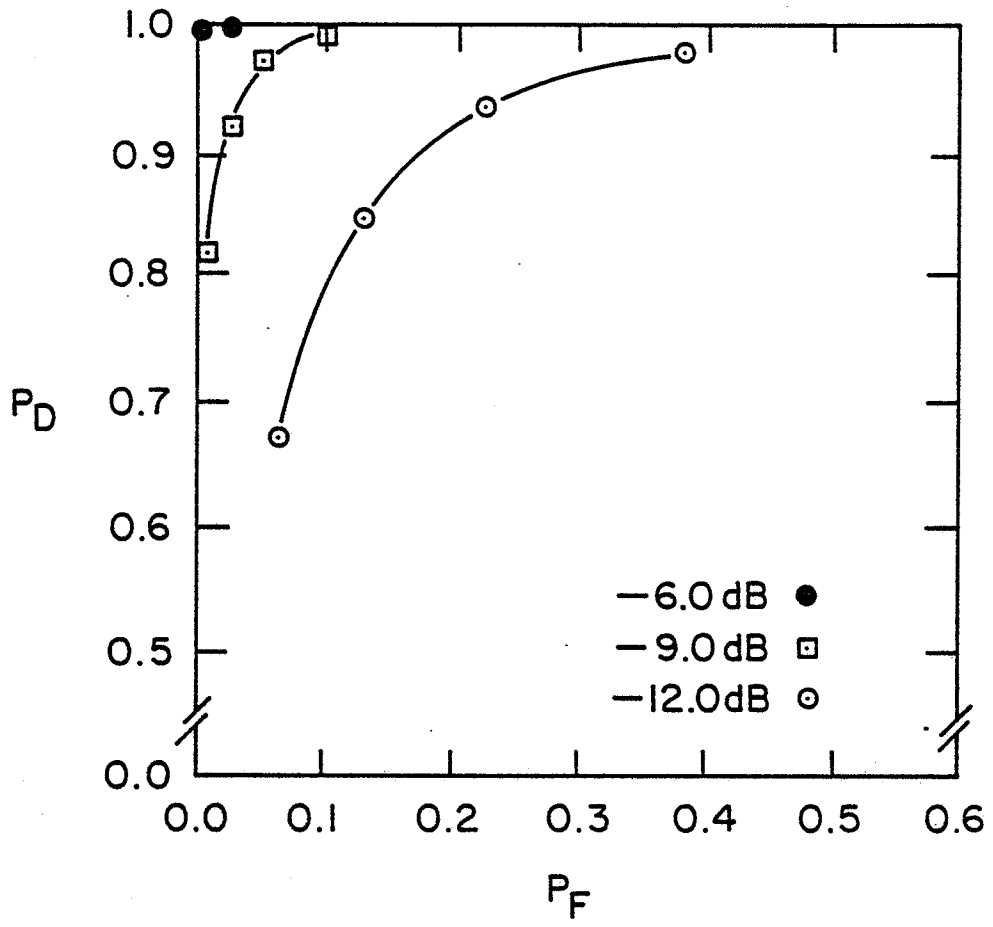

QRS detector:	Matched filter (h(t) prewhitened for a 1:16, Artifact to EMG power ratio)
Heart signal:	180 BPM reference
Noise:	1:16, Artifact to EMG power

Fig. 4.7(a) Noise PDS variation ROC curves

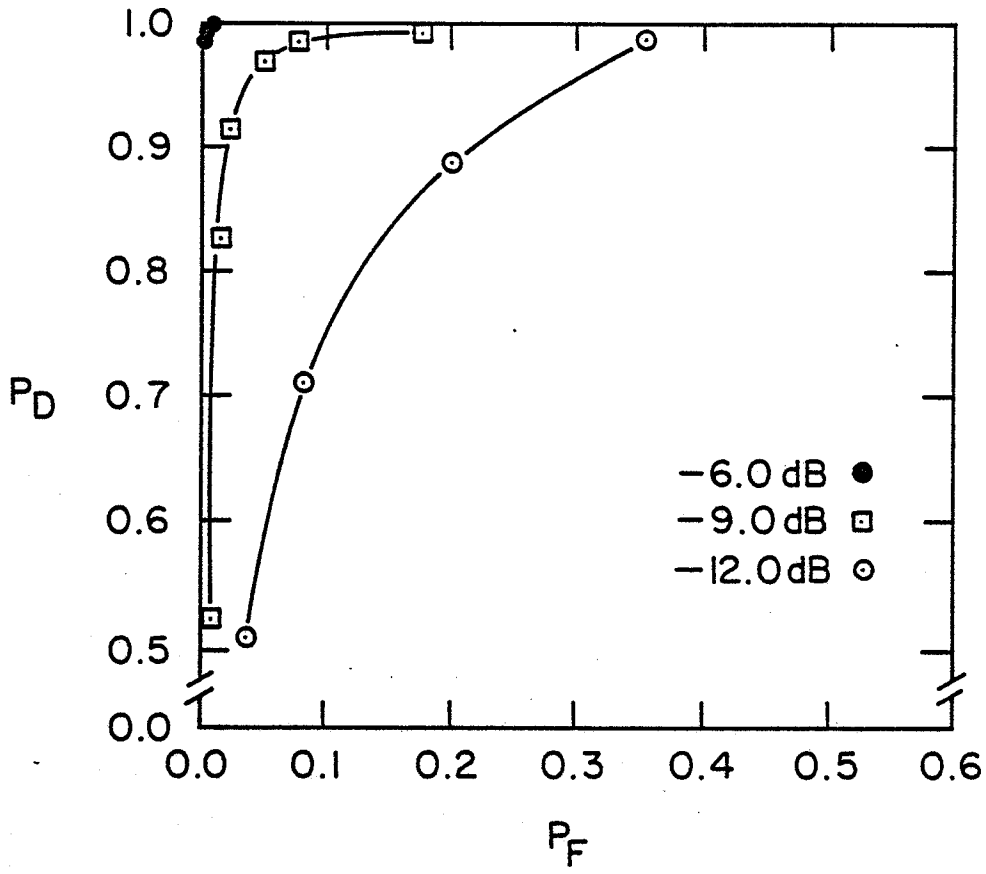

QRS detector:	Matched filter (h(t) prewhitened for a 1:4, Artifact to EMG power ratio)
Heart signal:	180 BPM reference
Noise:	1:4, Artifact to EMG power

Fig. 4.7(b) Noise PDS variation ROC curves

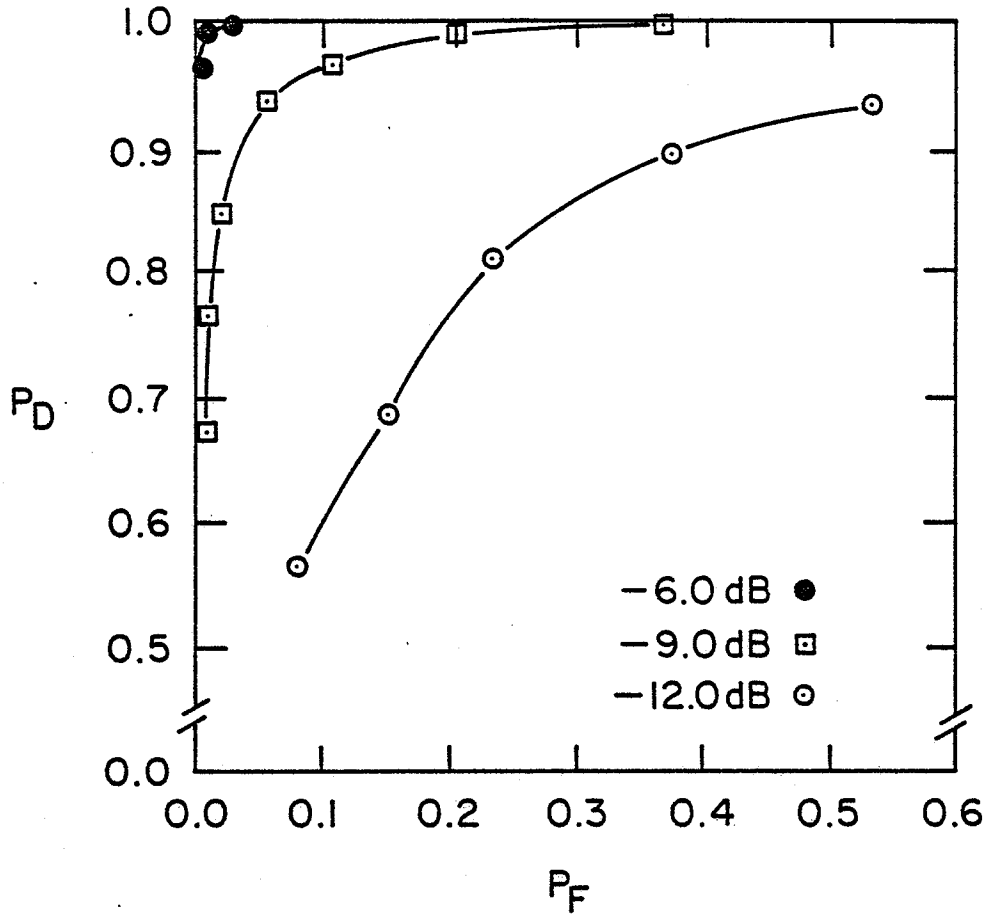

QRS detector:	Matched filter (h(t) prewhitened for a 4:1, Artifact to EMG power ratio)
Heart signal:	180 BPM reference
Noise:	4:1, Artifact to EMG power

Fig. 4.7(c) Noise PDS variation ROC curves

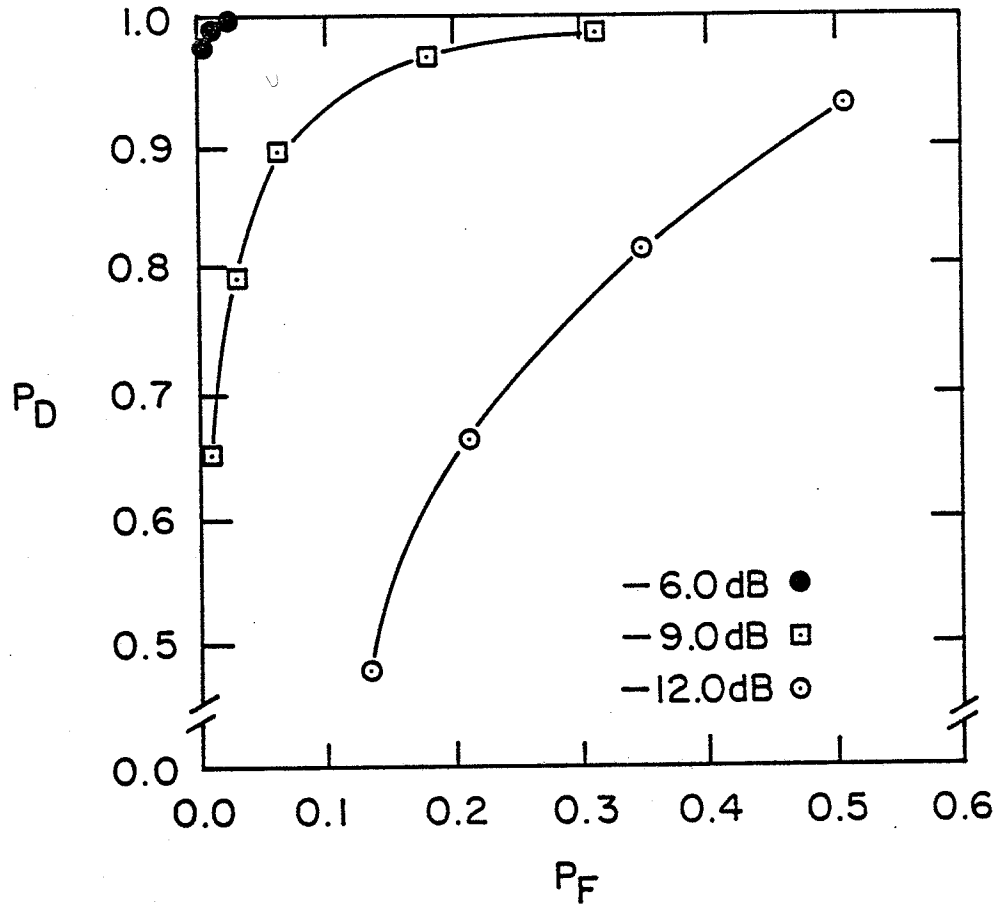

QRS detector:	Matched filter (h(t) prewhitened for a 16:1, Artifact to EMG power ratio)
Heart signal:	180 BPM reference
Noise:	16:1, Artifact to EMG power

Fig. 4.7(d) Noise PDS variation ROC curves

4.4 Performance Sensitivity to Heart Signal Shape

The matched filter QRS detector performance sensitivity to heart signal mismatch was evaluated by creating five different FIR specifications (h(t)) derived from five different heart signals (Appendix D), prewhitened for equal artifact and muscle noise. ROC curves were then generated by testing the five matched filters with 180 BPM reference heart signal and equal component noise. Performance table 4.4 summarizes the results of the ROC curves of Fig. 4.8 and 4.9.

Matched Signal	Test Signal	Operating Point P_D	P_F	S/N (dB)
180 ref	180 ref	0.95	0.05	-9.0
$S_1(t)$	180 ref	0.92	0.09	-9.0
$S_2(t)$	180 ref	0.91	0.09	-9.0
$S_3(t)$	180 ref	0.89	0.12	-9.0
$S_4(t)$	180 ref	0.92	0.10	-9.0
$S_5(t)$	180 ref	0.90	0.11	-9.0
$S_5(t)$	180 $S_5(t)$	0.90	0.10	-9.0

Table 4.4

Heart Signal Sensitivity Performance Summary

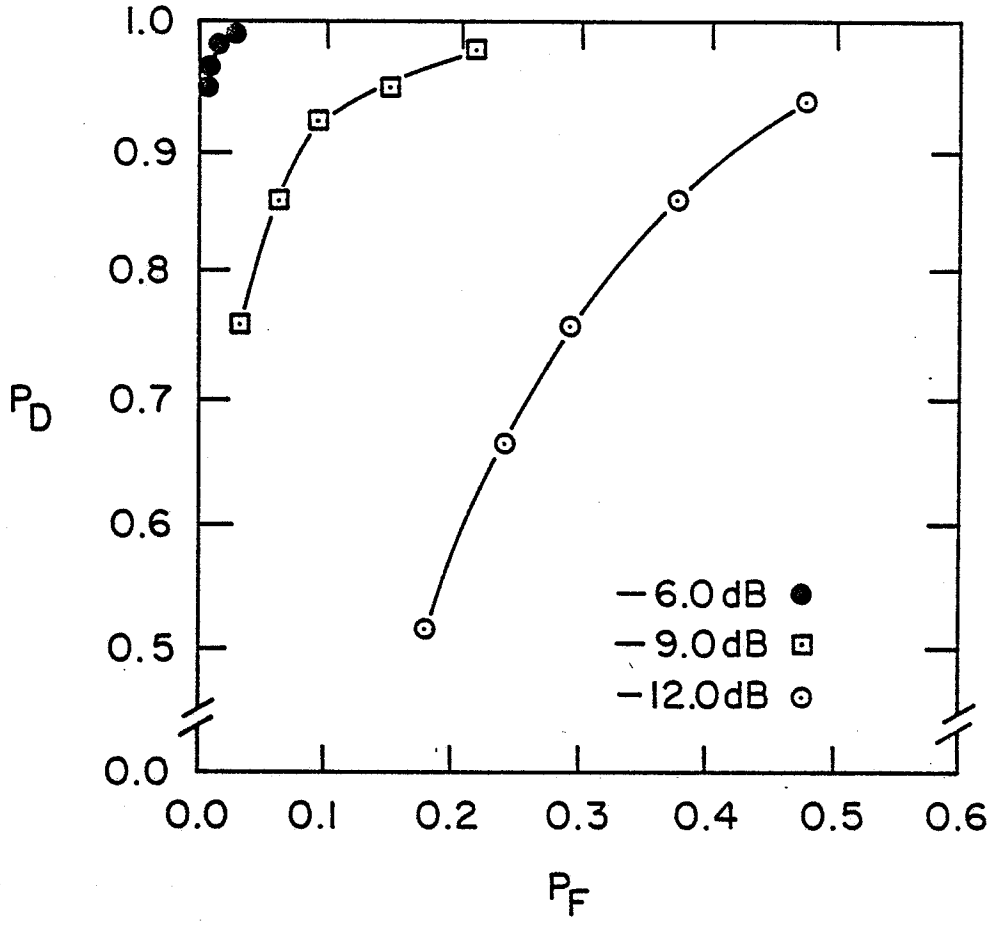

QRS detector: Matched filter (h(t) prewhitened to a 1:1, Artifact to EMG power ratio)

Heart signal: $s_1(t)$
(h(t) matched to 180 BPM reference)

Noise: 1:1, Artifact to EMG power

Fig. 4.8(a) Heart signal sensitivity ROC curves

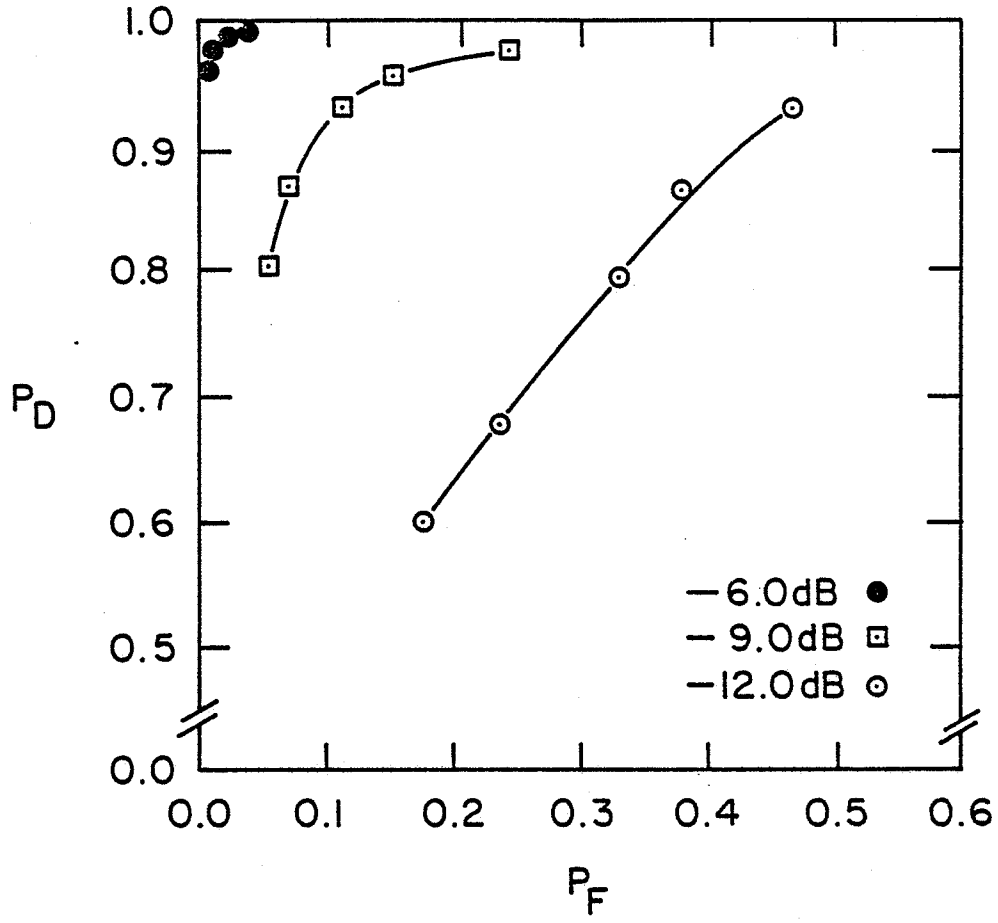

QRS detector:	Matched filter (h(t) prewhitened to a 1:1, Artifact to EMG power ratio)
Heart signal:	$s_2(t)$ (h(t) matched to 180 BPM reference)
Noise:	1:1, Artifact to EMG power

Fig. 4.8(b) Heart signal sensitivity ROC curves

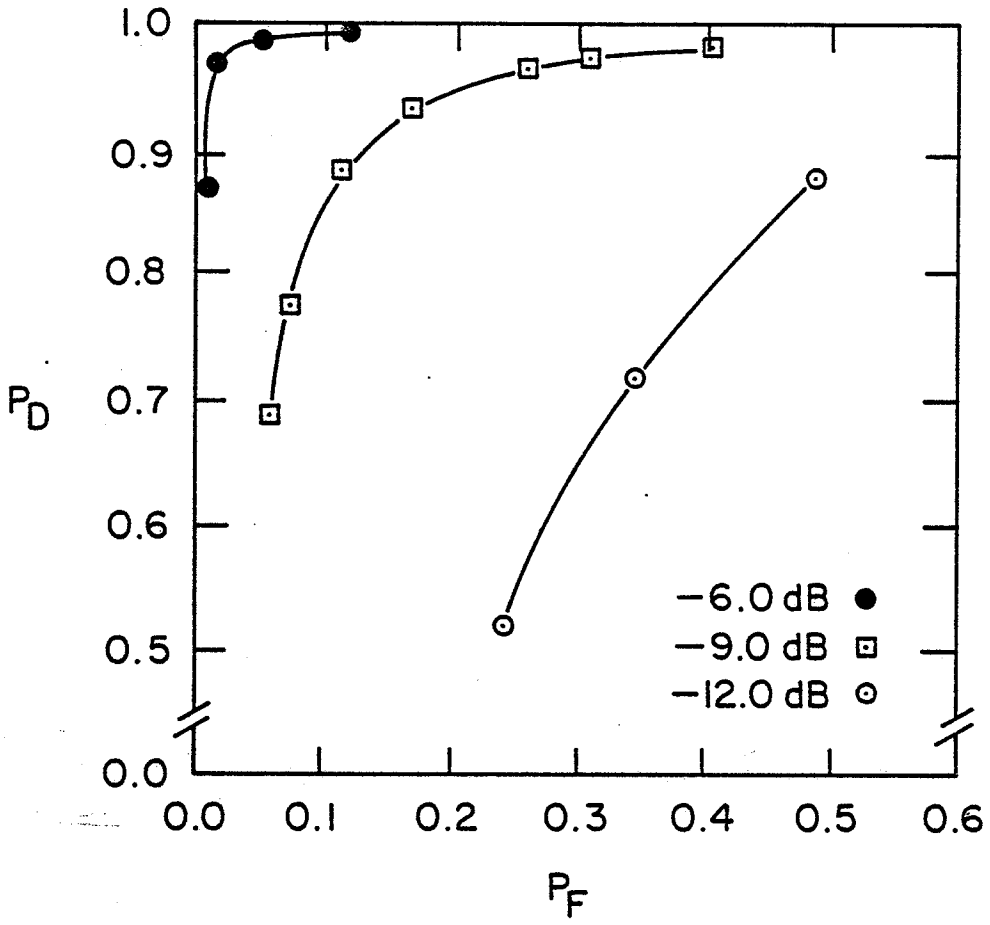

QRS detector: Matched filter (h(t) prewhitened to a 1:1, Artifact to EMG power ratio)

Heart signal: $s_3(t)$
(h(t) matched to 180 BPM reference)

Noise: 1:1, ARtifact to EMG power

Fig. 4.8(c) Heart signal sensitivity ROC curves

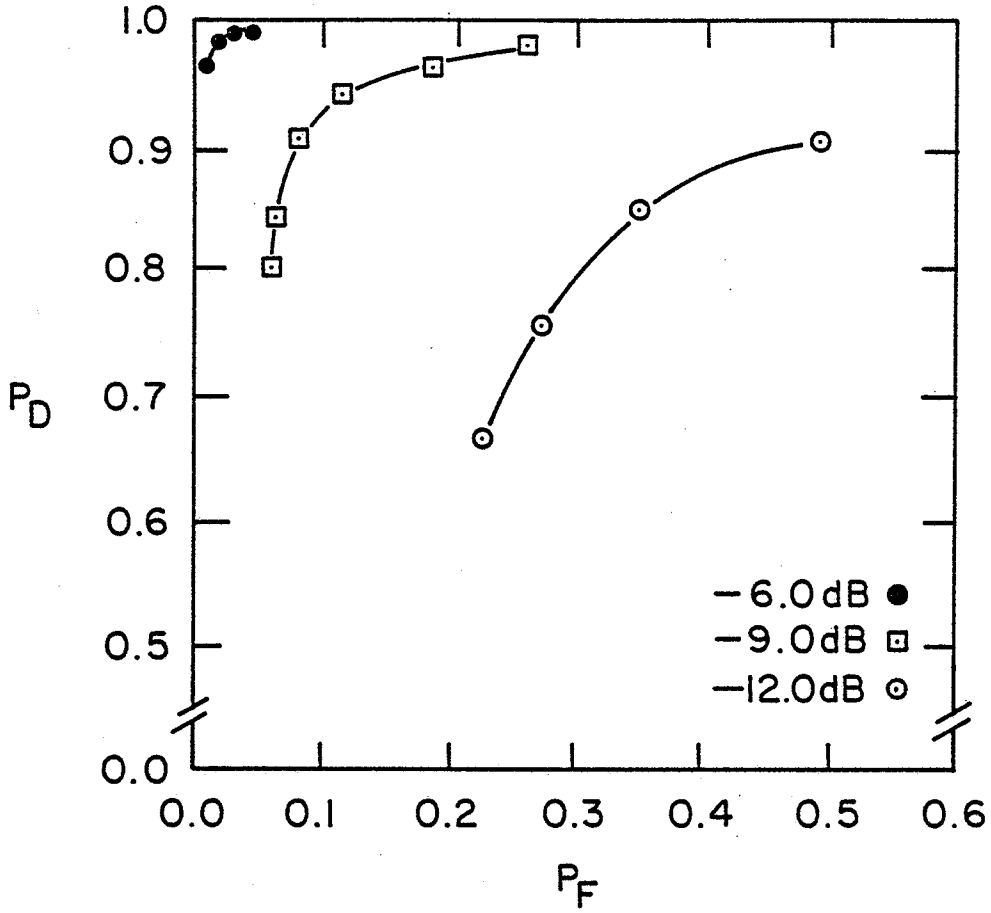

QRS detector:	Matched filter (h(t) prewhitened for a 1:1, Artifact to EMG power ratio)
Heart signal:	$s_4(t)$ (h(t) matched to 180 BPM reference)
Noise:	1:1, Artifact to EMG power

Fig. 4.8(d) Heart signal sensitivity to ROC curves

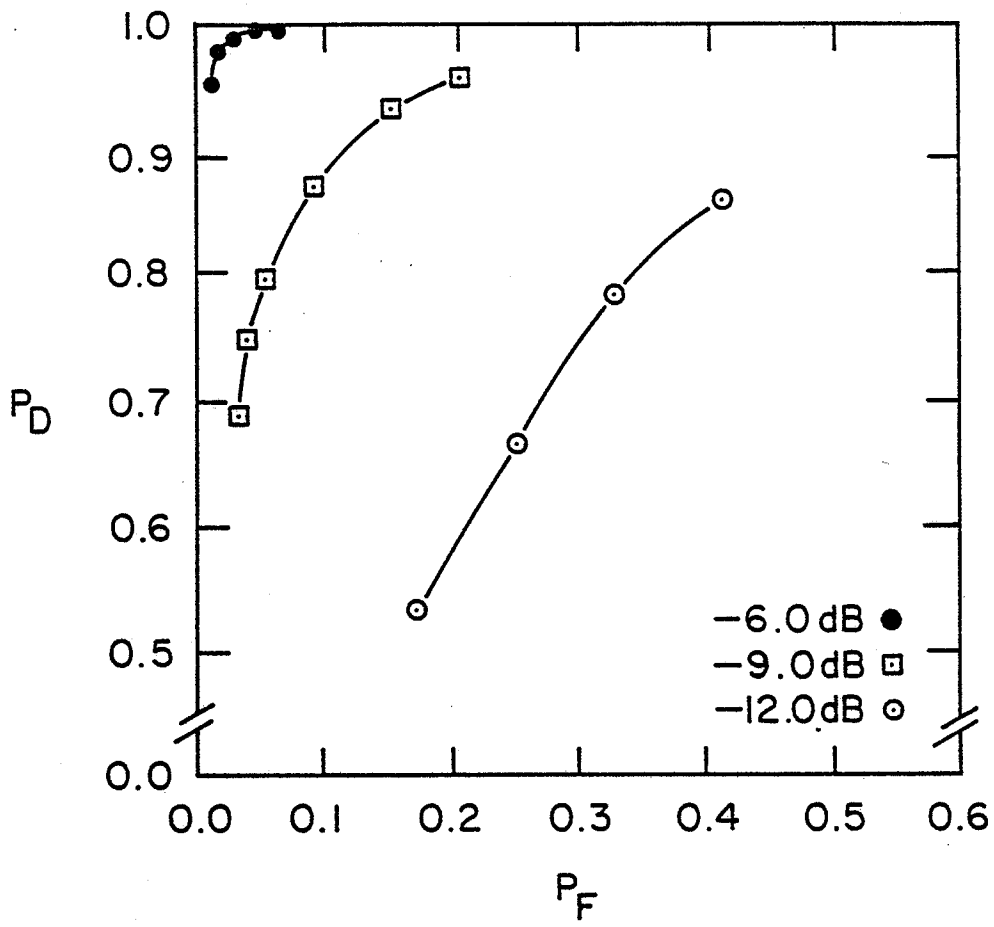

QRS detector:	Matched filter (h(t) prewhitened for a 1:1, Artifact to EMG power ratio)
Heart signal:	$s_5(t)$ (h(t) matched to 180 BPM reference)
Noise:	1:1, Artifact to EMG power

Fig. 4.8(e) Heart signal sensitivity ROC curves

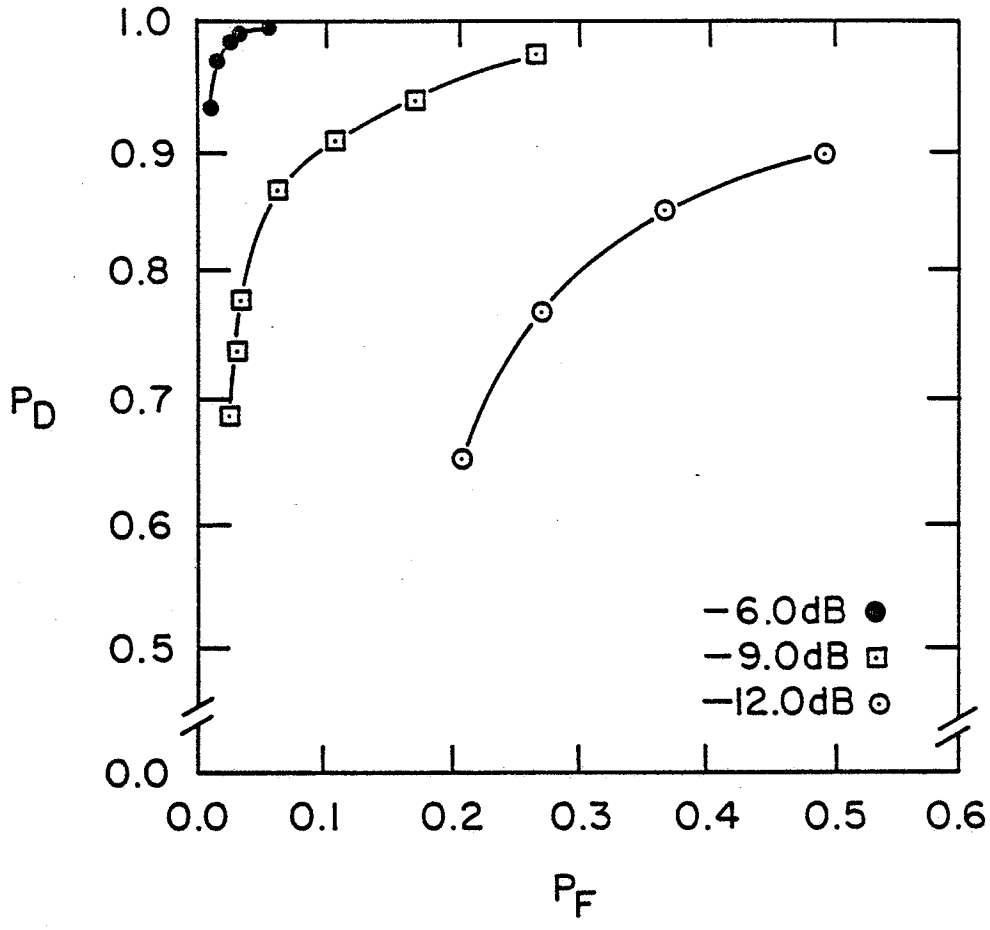

QRS detector:	Matched filter ($h(t)$ prewhitened for a 1:1, Artifact to EMG power ratio)
Heart signal:	$s_5(t)$ ($h(t)$ matched to $s_5(t)$
Noise:	1:1, Artifact to EMG power

Fig. 4.8(f) Heart signal sensitivity ROC curves

In the last entry of table 4.4, one of the poorest FIR h(t), was retested with the signal to which it was matched. The performance did not improve significantly. This demonstrates that the maximum performance is signal shape dependent as indicated in the coloured noise detection problem described in [11].

4.5 Other Tests

Two other tests were performed. The FIR 180 beat reference filter weights for the matched filter prewhitened with equal power noise components were reduced from 8 bits to 4 bits. The -9.0 S/N curve of the ROC was checked and found to coincide exactly with the 8 bit version. This was to investigate performance sensitivity to word length used in the digital realization of the matched filter.

The second test involved testing the Winter-Trenholm QRS detector with the 200 BPM version of the $s_5(t)$ sensitivity heart signal. The ROC curve is included in Fig. 4.9. There was about a 1.5 dB degradation in performance.

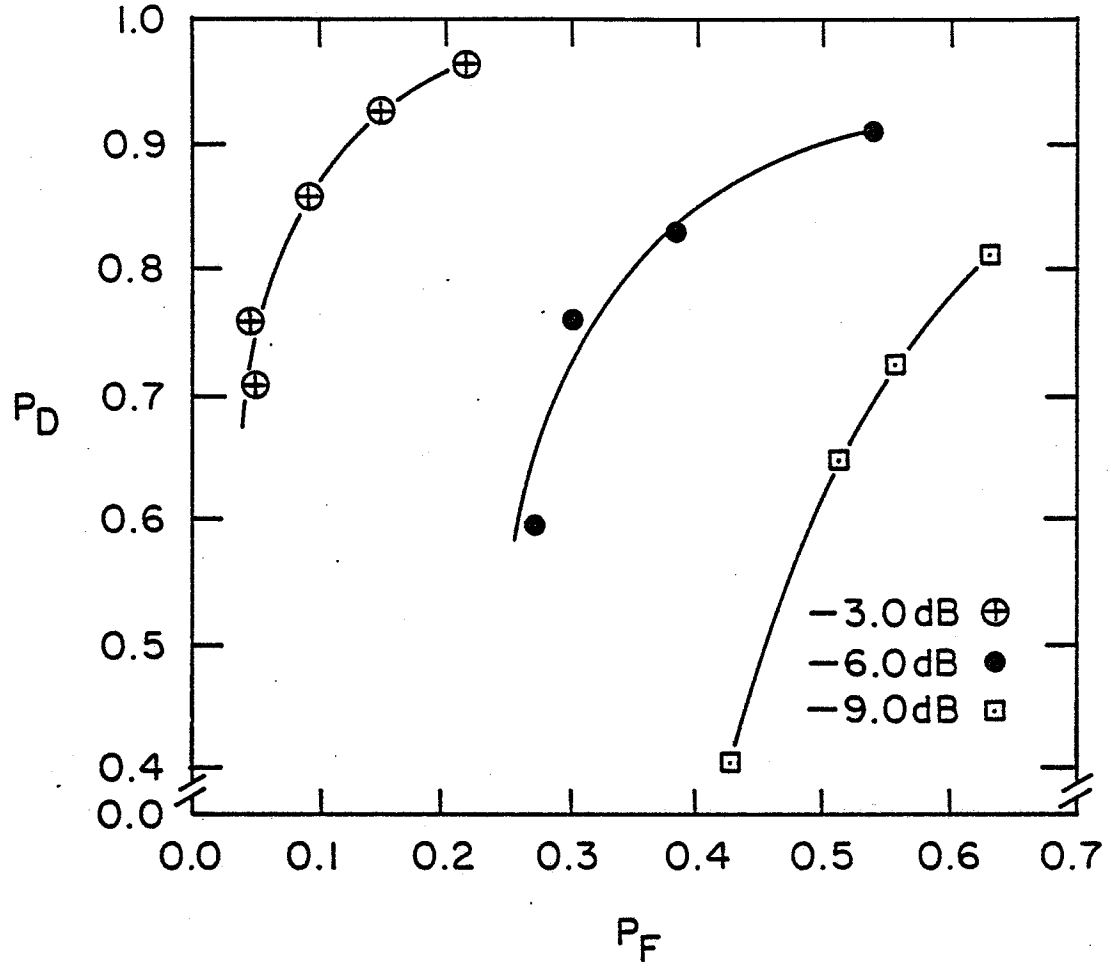

QRS detector: Winter-Trenholm prototype

Heart signal: $S_5(t)$

Noise: 1:1, Artifact to EMG power

Fig. 4.9 Winter-Trenholm prototype heart signal sensitivity ROC curves

CHAPTER V

CONCLUSIONS, OBSERVATIONS AND RECOMMENDATIONS

5.1 Conclusions

The results of Chapter IV indicate that the matched filter QRS detector is reliable. Within the bounds of the modelling assumptions and the other QRS detector types tested, the matched filter QRS detector proved to be the best performer as suggested by signal detection theory. It has a 6dB S/N performance improvement over the Winter-Trenholm detector as shown in Table 4.3. Implementation of the matched filter detector is feasible with a straight forward digital structure. Threshold is the only adjustment required for obtaining optimum performance. This adjustment has the potential to be set automatically, requiring no attention by the user. Sensitivity to signal shape and noise PDS variation did not appear to be critical. On the basis of these findings, it is concluded that the matched filter is a useful approach to QRS detector design, using present day standard digital LSI (large scale integration) semiconductor devices such as microprocessors.

5.2 Some Other Observations

The formulation of the problem, its solution, realization and experimental verification provided some insight into the concepts of QRS detection. For example, prewhitening may be viewed as processing the signal with a bandpass filter determined by the noise PDS. The resulting output signal is processed by a matched filter prior to threshold detection. This is simply inserting a correlator in between the bandpass filter and the comparator used in many existing QRS detectors. The effect of the correlator is to convert a portion of the signal into one parameter for subsequent threshold comparison. As a result, the QRS detector response is delayed by the time period of the correlation waveform. Although the time delay is consistent and predictable, it is the penalty paid for improved performance. The Winter-Trenholm detector also had a delayed decision characteristic, though not as severe (22 mS).

Prediction of the optimum threshold for the matched filter QRS detector was not formally investigated. However, it was noted that in real situations, the level of the heart signal is modulated by the respiratory cycle (breathing). This multiplicative noise was not included the model of heart signal in noise used in this thesis. The respiratory variation would make the optimum threshold and signal to noise ratio time varying. The effect of the former introduces the requirement for minimizing detector performance sensitivity

to optimal threshold setting deviations and determining electrode placements that minimize respiratory effects. The optimum threshold setting for the stationary case is predicted by signal detection theory to be one half the square root of the power of the prewhitened signal. A microprocessor based matched filter QRS detector could easily determine the optimum setting in a learn mode, operating initially on the clean ECG of the subject at rest using an algorithm based on the theory.

The matched filter used a nonrecursive transversal implementation that requires many arithmetic operations to implement digitally. The two features of the transversal filter needed for a matched filter are independently specifiable amplitude and phase characteristics and direct synthesis from the time domain specification. It may be feasible to use a much simpler recursive structure to implement the matched filter with specified magnitude and phase characteristics.

The matched filter is the optimum technique for the detection of QRS waves in Gaussian noise. Usually, the timing of the successively detected heart signals is used to calculate heart rate. Another approach would be to use optimum techniques for estimating a parameter of a signal corrupted by noise. The parameter of interest being heart rate. A suggested approach is to use a phase locked loop by taking the point of view that a PLL (phase locked loop) maximizes the correlation between the input signal and the VCO

(voltage controlled oscillator) signal. The degree of maximum correlation to the signal and minimum correlation to the noise may be enhanced by using a VCO waveform that corresponds to the impulse response of the matched filter. If the dynamics of the loop and the signal allow a stable realization, what will result is a QRS detector with the ability to correlate to a longer signal length consisting of many PQRST waves with a corresponding S/N improvement. The problem is no longer modelled as a binary signal in noise, but as an infinite set of periodic signals in noise each distinguished by its frequency (heart rate). The new model and heart rate estimator are shown in Fig. 5.1. The PLL scheme includes a matched filter.

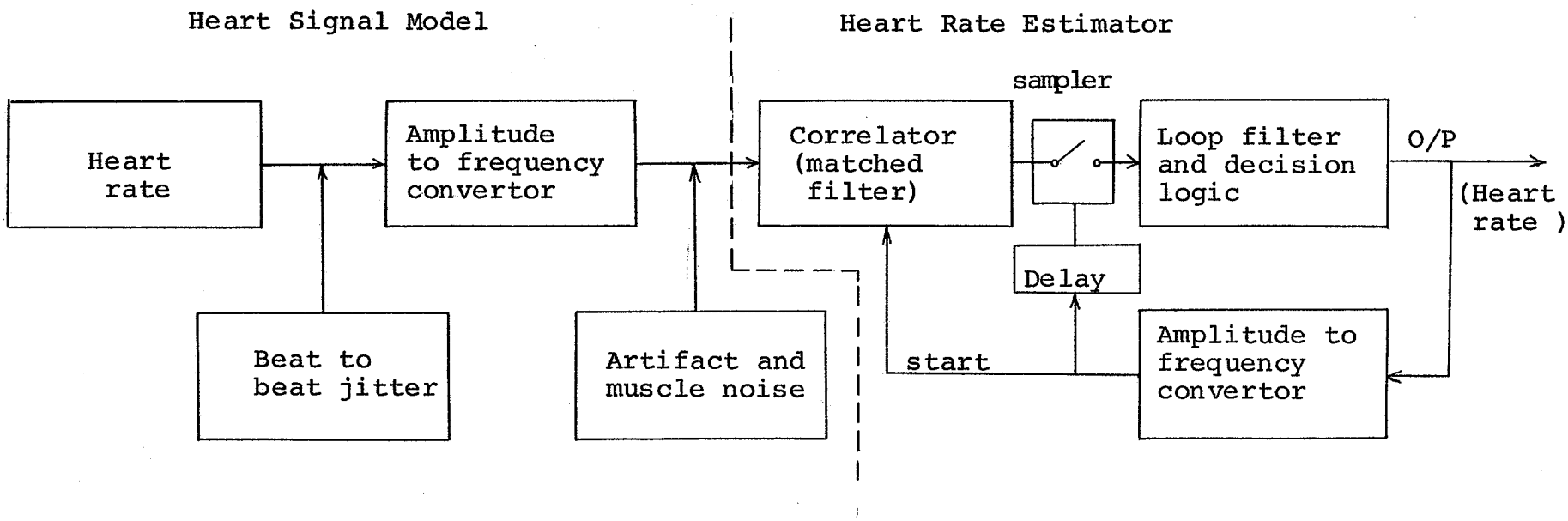

Fig. 5.1 Estimation of heart rate in noise.

5.3 Recommendations

The approach used in this thesis to design, implement and test an 'optimum' QRS detector based on a matched filter is rather academic. The question remains whether it will perform in real situations in a practical and useful form. This leads back to subjective testing and evaluation by users. Since a complete minicomputer is not a convenient or economically justifiable device to use as a portable heart beat detector for user evaluation, it is recommended that a portable prototype be developed for trial purposes. It is hoped that sufficient information and data is presented in this thesis to support the prototype design. It is also recommended that the proposed matched filter PLL heart rate measurement technique be investigated.

APPENDIX A

CALCULATION OF MATCHED FILTER RESPONSE

The detailed procedure used for calculating the optimum h(t) specified by equation 2.12 as outlined in Fig. 2.9 is as follows:

(1) Create the basic floating point data files 'NEMG', and 'NART' by using equations 2.1 and 2.3 respectively to specify from 0 - 250 Hz, the first 513 points of each 1024 element file. The remaining 511 elements of each file are the 'reflections' of their first 512 elements less their respective first elements 'mirrored' about the centre points.

(2) Sample at 500 Hz, digitize, and store the desired heart signal in a 1024 element integer buffer by employing the AAD command of the DEC signal processing program called SPARTA. Display the digitized heart signal. Subtract 2048 from the SPARTA integer buffer in which the heart signal is stored to remove the 'numerical off set' from the 12 bit A/D converter. Locate a suitable noise free PQRST complex and rotate it to the beginning of the buffer with the BAL command. In order to maintain resolution in the frequency domain, the complex should occupy no more than the first 25% of the 1024 element. The remainder of the heart signal buffer must be zeroed.

(3) Perform the digital Fourier transform of the heart signal using the FFT command. The real and imaginary components of the transform will each require a 1024 integer buffer. Create floating point versions of these buffers with the BMO command in preparation for prewhitening by 'NEMG' and 'NART'.

(4) Create a total noise PDS floating buffer by adding the noise components from the 'NART' and 'NEMG' data files in the desired ratio. Take the reciprocal of each element of this new buffer. Multiply the floating point heart signal transform buffers (both real and imaginary) by the total noise PDS reciprocal buffer using the BMU command. Convert the resulting heart signal transform buffers back into integer buffers.

(5) Take the inverse discrete Fourier transform of the resulting prewhitened heart signal buffers. The result is the desired matched filter response h(t) in discrete form.

(6) Create a data file for the transversal filter operating at 250 Hz with 8 bit weights by scaling the peak value of h(t) to $\pm$ 127 (decimal) and using every second point in the non zero portion of the response. The resulting set of weights should number less than 100.

APPENDIX B

Instrumentation Summary

True RMS level meters - H/P (Hewlett-Packard) 3400A

Instrumentation tape recorder - H/P 3960A

Level reference oscillator - Wavetek

Gaussian noise generator - H/P 3722A

Beat counters - Advance Instruments TC9A and TC9B

QRS detector evaluation - U of M QRS detector test set

APPENDIX C

QRS Detector Program

The matched filter QRS detector computer program follows. It is a combined source and object code listing for a DEC PDP 11/40 equipped with a LPS (laboratory peripheral system) and a hardware floating point arithmetic unit.

```
1                       ;MATCHED FILTER QRS DETECTOR
2                       .MCALL  .REGDEF,.EXIT,..V2..,.PRINT,.SRESET,.CLOSE
3 000000                ..V2..
4 000000                .REGDEF
5         000051 HYS=41.
6         000132 PTS=90.
7 000000 010706 A0:     MOV     PC,SP
8 000002 005746         TST     -(SP)
9 000004                .SRESET
10 00006 012700         MOV     #AREA,R0
         001524'
11 00012 012710         MOV     #400,(R0)
         000400
12 00016 112710         MOVB    #0,(R0)
         000000
13 00022 012760         MOV     #FILNAM,2(R0)
         001536'
         000002
14 00030 005060         CLR     4(R0)
         000004
15 00034 104375         EMT+375
16 00036 103001         BHIS    A4
17 00040 000000         HALT                    ;FILE INPUT ERROR
18 00042 012700 A4:     MOV     #AREA,R0
         001524'
19 00046 012710         MOV     #4000,(R0)
         004000
20 00052 112710         MOVB    #0,(R0)
         000000
21 00056 012760         MOV     #0,2(R0)
         000000
         000002
22 00064 012760         MOV     #WTS,4(R0)
         000564'
         000004
23 00072 012760         MOV     #PTS,6(R0)
         000132
         000006
24 00100 012760         MOV     #0,10(R0)
         000000
         000010
25 00106 104375         EMT+375
26 00110                .CLOSE #0
27 00122 103001         BHIS    3$
28 00124 000000         HALT                    ;I/O ERROR
29 00126 005067 3$:     CLR     AREA
         001372
30 00132 012703         MOV     #PTS,R3
         000132
31 00136 012705         MOV     #WTS,R5
         000564'
32 00142 006215 A7:     ASR     (R5)
33 00144 006215         ASR     (R5)
34 00146 006215         ASR     (R5)
35 00150 006215         ASR     (R5)
36 00152 005515         ADC     (R5)
37 00154 012546         MOV     (R5)+,-(SP)
38 00156 077307         SOB     R3,A7
39 00160 012705         MOV     #WTS,R5
         000564'
40 00164 012703         MOV     #PTS,R3
         000132
41 00170 012625 A8:     MOV     (SP)+,(R5)+
42 00172 077302         SOB     R3,A8
43 00174 012767         MOV     #404,170404     ;SET CLKSTAT,100KHZ,RPT
         000404
         170404'
44 00202 012767         MOV     #-400.,170406   ;PRESET CLK
         177160
         170406'
45 00210 012767         MOV     #40,170400
         000040
         170400'
46 00216 013700         MOV     @#170402,R0
         170402
47 00222 005267         INC     170404
         170404'
48 00226 012706         MOV     #DLY,SP         ;PC POINTS TO DELAY(0)
         001144'
49 00232 005767 A9:     TST     170400
         170400'
50 00236 100001         BPL     1$              ;AD NOT READ ERROR
51 00240 000000         HALT
52 00242 105767 1$:     TSTB    170400  ;AD READY?
         170400'
53 00246 100375         BPL     1$
54 00250 010467         MOV     R4,170420       ;O/P TO XDA
         170420'
55 00254 016700         MOV     170402,R0       ;I/P SAMPLE TO MULTIPLIER
         170402'
56 00260 072027         ASH     #-4,R0          ;12 TO 8 BITS
         177774
57 00264 005500         ADC     R0
58 00266 162700         SUB     #200,R0
         000200
59 00272 012702         MOV     #DLY,R2         ;R2 WILL POINT TO PREVIOUS
         001144'
60 00276 010203         MOV     R2,R3           ;R3 POINTS TO DELAY
61 00300 012704         MOV     #WTS,R4         ;R4 POINTS TO WEIGHTS
         000564'
```

```
62 00304 012401 B6:     MOV     (R4)+,R1        ;NEXT TO WEIGHT TO MULTIPLICAND
63 00306 070100         MUL     R0,R1
64 00310 006201         ASR     R1              ;TAP SCALE
65 00312 005501         ADC     R1              ;ADD ROUND OFF
66 00314 010123         MOV     R1,(R3)+        ;PRODUCT TO NEXT DELAY
67 00316 022704         CMP     #WTS+<PTS*2>,R4 ;LAST TAP?
         001050'
68 00322 001403         BEQ     B5
69 00324 061312         ADD     (R3),(R2)       ;SHIFT AND ADD DELAY
70 00326 005522         ADC     (R2)+
71 00330 000765         BR      B6
72 00332 011604 B5:     MOV     (SP),R4         ;FILTER O/P
73 00334 072427         ASH     #-4,R4          ;16 TO 12 BITS
         177774
74 00340 005504         ADC     R4
75 00342 062704         ADD     #4000,R4        ;RESTORE AD OFFSET
         004000
76 00346 005737         TST     @#177570        ;SET THRESHOLD? (MSB CONSOLE SE
         177570
77 00352 100051         BPL     6$
78                      ;
79                      ;COMPARATOR,  R5=THRESHOLD  AREA=COMP O/P 0/1
80                      ;BINARY TO BCD FOR LED OF THRESHOLD VALUE
81                      ;R2 CONTAINS #, R0,R1 ALSO USED
82                      ;
83 00354 105237         INCB    @#170401        ;AD TO CHANNEL #1
         170401
84 00360 105737 8$:     TSTB    @#170400        ;AD RDY?
         170400
85 00364 100375         BPL     8$
86 00366 013701         MOV     @#170402,R1     ;# TO DIVIDEND
         170402
87 00372 010105         MOV     R1,R5           ;STORE THRESHOLD
88 00374 005067         CLR     AREA            ;AREA=LED WORD FOR ADBUF WRITE
         001124
89 00400 005000 4$:     CLR     R0
90 00402 071027         DIV     #10.,R0         ;R0 IS QUOTIENT,R1 REMAINDER
         000012
91 00406 110167         MOVB    R1,AREA         ;SET UP DIGIT
         001112
92 00412 016737         MOV     AREA,@#170402   ;LOAD DIGIT
         001106
         170402
93 00420 105267         INCB    AREA+1          ;NEXT DIGIT
         001101
94 00424 010001         MOV     R0,R1           ;MOV QUOT.  TO DIV.
95 00426 001364         BNE     4$              ;DIV.  0?
96 00430 112767         MOVB    #13,AREA        ;BLANK LOADED
         000013
         001066
97 00436 016737 5$:     MOV     AREA,@#170402   ;LOAD BLANK
         001062
         170402
98 00444 105267         INCB    AREA+1          ;NEXT DIGIT
         001055
99 00450 022767         CMP     #3000,AREA      ;ANY DIG'S TO 0
         003000
         001046
100 0456 101367         BHI     5$              ;FINISHED LED DISPLAY
101 0460 005737         TST     @#177570        ;RUN FILTER? (MSB CONSOLE
         177570
102 0464 100735         BMI     8$
103 0466 105337         DECB    @#170401        ;RESTORE ADSTAT CH #0
         170401
104 0472 005067         CLR     AREA
         001026
105 0476 012767 6$:     MOV     #4000,170422    ;RESET YDA TO 0 V.
         004000
         170422'
106 0504 005767         TST     AREA            ;COMP O/P 0?
         001014
107 0510 001414         BEQ     1$              ;IF 0 GOTO SET COMPARISON
108 0512 062704         ADD     #HYS,R4         ;RESET LEVEL -0.1V SET LEVE
         000051
109 0516 020405         CMP     R4,R5           ;RESET COMPARISON
110 0520 003005         BGT     9$              ;NO RESET,  CONT FILT
111 0522 162704         SUB     #HYS,R4
         000051
112 0526 005067         CLR     AREA            ;RESET COMP
         000772
113 0532 000637         BR      A9              ;CONT FILT
114 0534 162704 9$:     SUB     #HYS,R4
         000051
115 0540 000634         BR      A9
116 0542 020405 1$:     CMP     R4,R5           ;SET COMPARISON
117 0544 003632         BLE     A9              ;NO SET,CONT FILT
118 0546 012767         MOV     #7777,170422    ;SET COMP &SET YDA
         007777
         170422'
119 0554 005267         INC     AREA
         000744
120 0560 000624         BR      A9
121 0562                .EXIT
122 0564         WTS:   .BLKW 120.
123 1144         DLY:   .BLKW 120.
124 1524         AREA:  .BLKW 5
125 1536 071126 FILNAM: .RAD50 /RK0RS0RSWDAT/
    1540 071611
    1542 071617
    1544 014474
```

```
126      000000'        .END A0

SYMBOL TABLE

AREA    001524R         A0      000000R         A4      000042R
A7      000142R         A8      000170R         A9      000232R
B5      000232R         B6      000304R         DLY     001144R
FILNAM  001536R         HYS   = 000051          PC    =%000007
PT5   = 000132          R0    =%000000          R1    =%000001
R2    =%000002          R3    =%000003          R4    =%000004
R5    =%000005          SP    =%000006          WTS     000564R
...V2 = 000001
```

APPENDIX D

Sensitivity Heart Signals

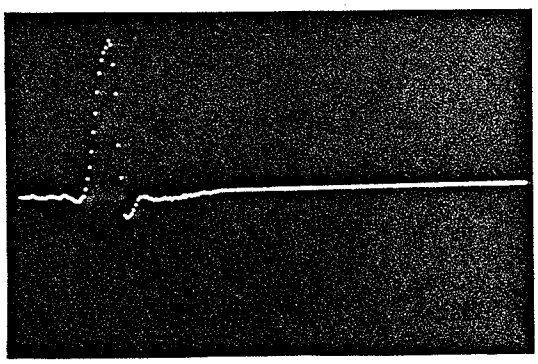

$s_1(t)$

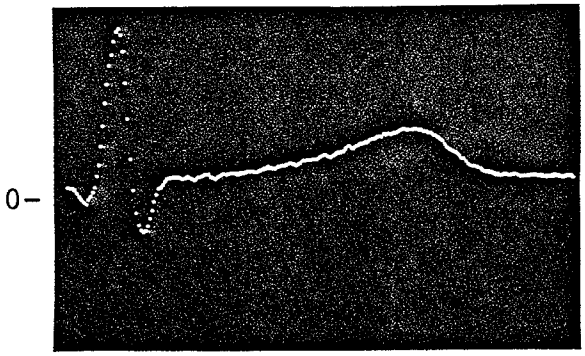

$s_2(t)$

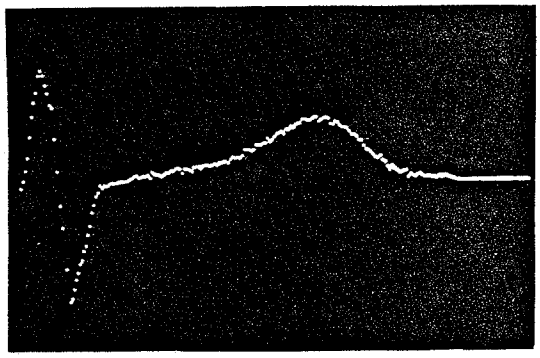

$s_3(t)$

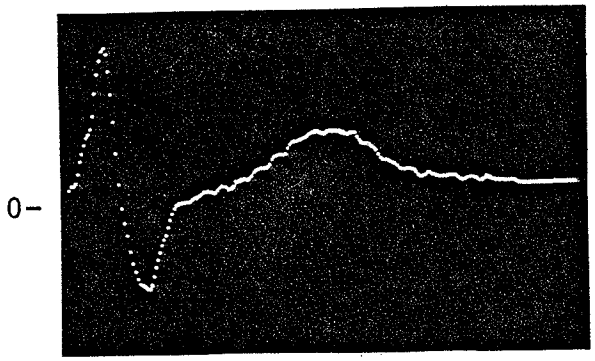

$s_4(t)$

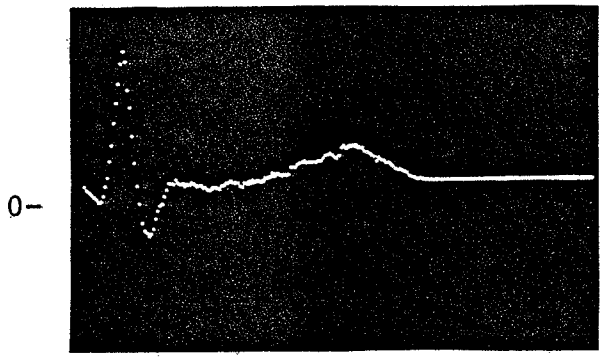

$s_5(t)$

Display of linear relative amplitude sampled at 500 Hz with a 450 mS duration.

180 BPM Reference h(t)'s prewhitened
by various noise PDS.

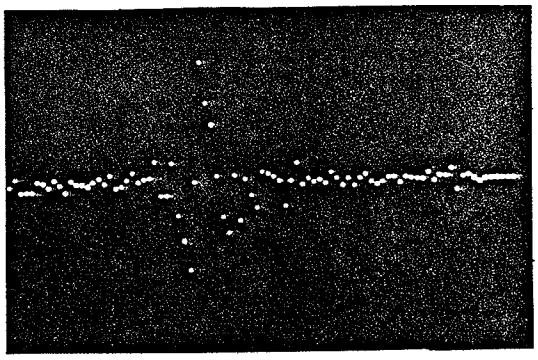

16:1 Artifact to EMG

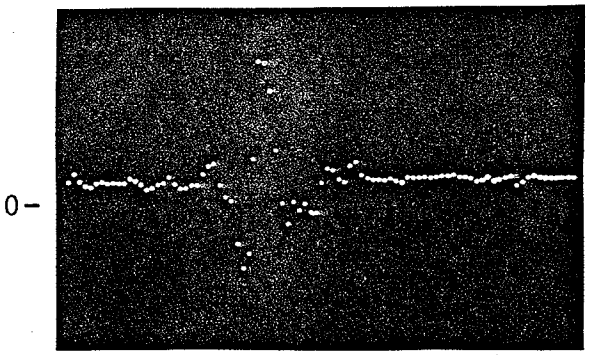

4:1 Artifact to EMG

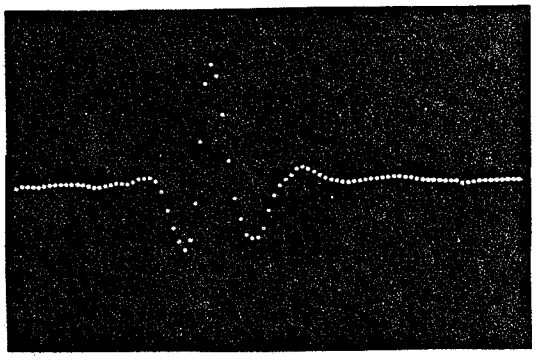

1:1 Artifact to EMG

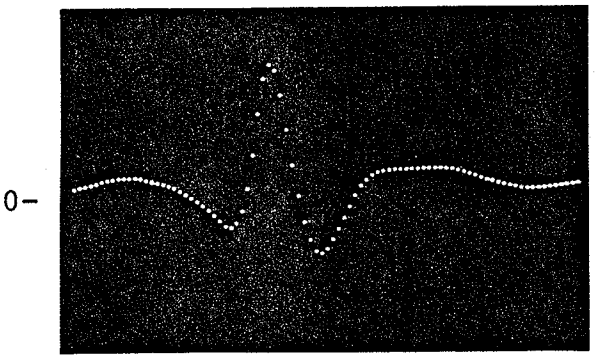

1:4 Artifact to EMG

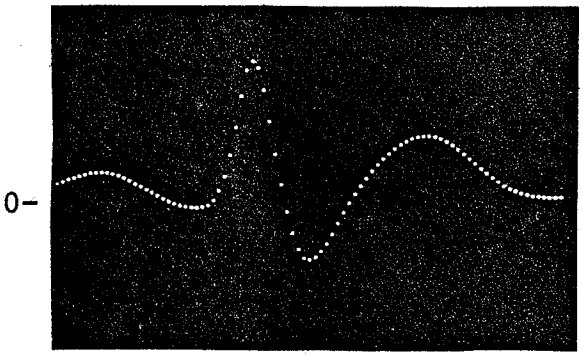

1:16 Artifact to EMG

All h(t)'s are 90 points with a 250 Hz sampling rate.

Sensitivity heart signal h(t)'s prewhitened for 1:1 Artifact to EMG noise power.

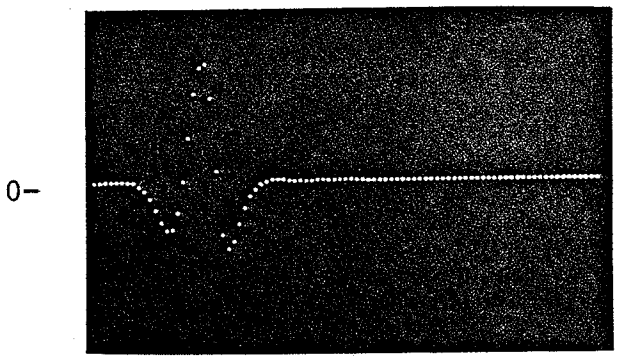

$h_1(t)$

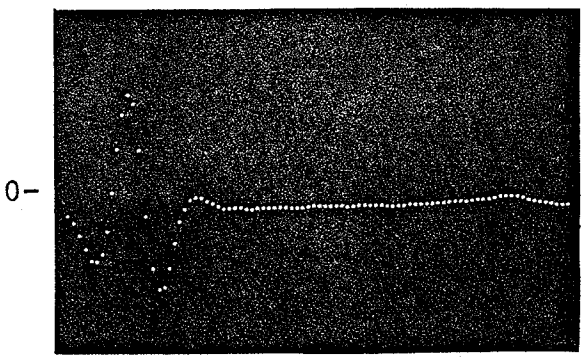

$h_2(t)$

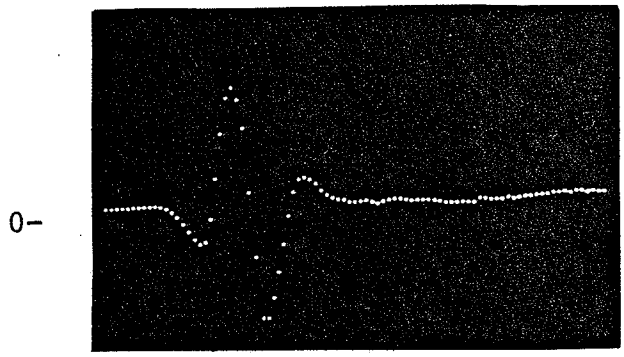

$h_3(t)$

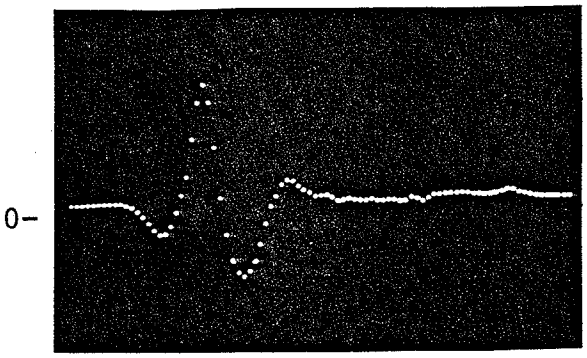

$h_4(t)$

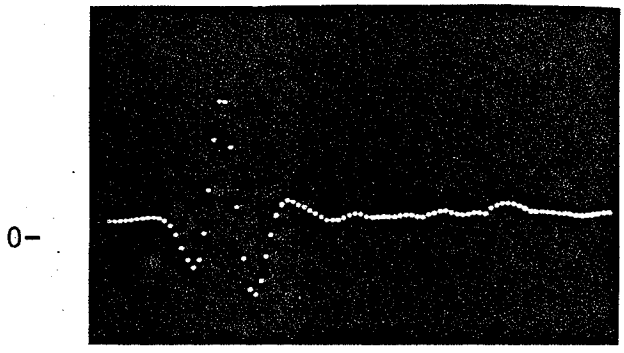

$h_5(t)$

All h(t)'s are 90 points at a 250 Hz sampling rate.

Prewhitening filter frequency response characteristics.

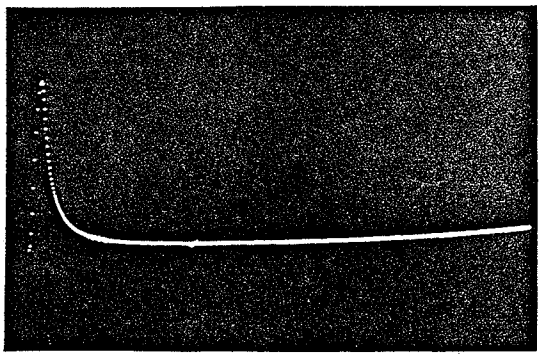

16:1 Artifact to EMG

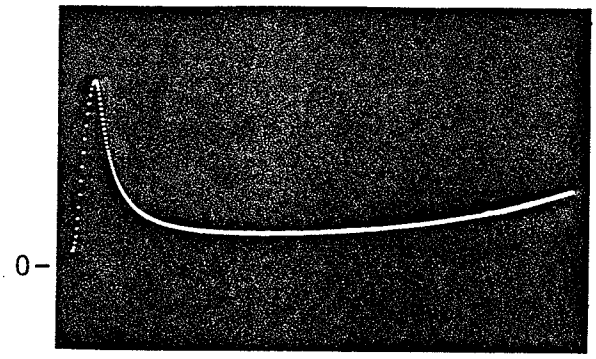

4:1 Artifact to EMG

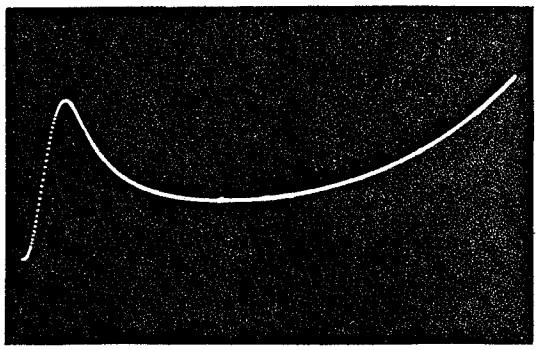

1:1 Artifact to EMG

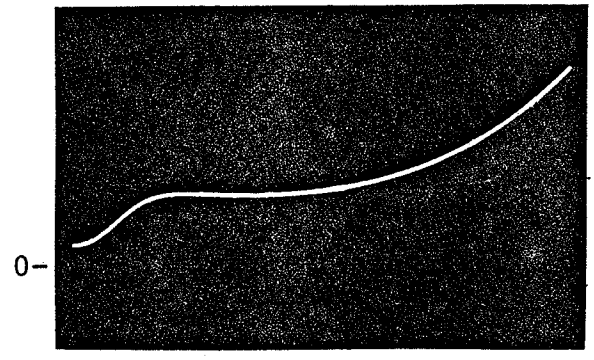

1:4 Artifact to EMG

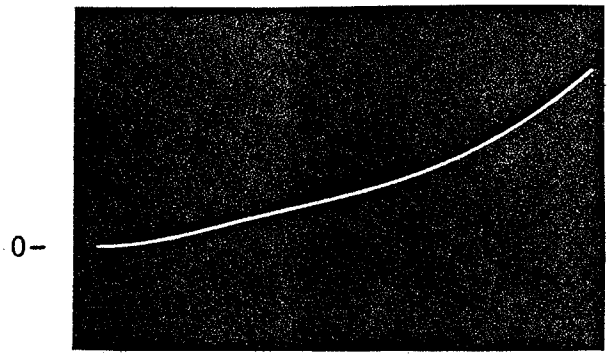

1:16 Artifact to EMG

Linear 0 to 250 Hz frequency response display of linear relative amplitude.

REFERENCES

[1] Hacke, M. and P. Vermeire. "A low-cost general purpose analogue QRS wave detector", MBE, November, 1974. pp. 823-826.

[2] Winter, D.A. and B.G. Trenholm. "Reliable Triggering for Exercise Electrocardiograms" IEEE Trans. BME-16, Number 1, January, 1969. pp. 75-76.

[3] Turin, G.L. "An Introduction to Matched Filters" IRE Trans. Inform. Theory, IT-6, pp. 311-326. June, 1960.

[4] Okajima, M. et al "Computer Pattern Recognition Techniques: Some Results with Real Electrocardiographic Data". IEEE Trans. BME, July, 1963. pp. 106-114.

[5] Hamby, A.R., R.L. Moruzzi, and C.L. Feldman. "The Use of Intrinsic Components in an ECG Filter" IEEE Trans. BME, November, 1974. pp. 469-473.

[6] Young, T.Y., and W.H. Huggins. "On the Representation of Electrocardiograms" IEEE Trans. BME, July, 1963. Vol. 10, pp. 86-95.

[7] Scott, R.N. "Technical Note: Myo-Electric Energy Spectra" Med & Biol. Engrg., Vol. 5, pp. 303-305, 1967.

[8] Parker, P.A. and R.N. Scott. "Statistics of the myoelectric signal from monopolar and bipolar electrodes." Medical and Biological Engineering, September, 1973. pp. 591-596.

[9] Shwedyk, E. "Estimation of a Muscle's force from its Myo-electric signal during quasi-isometric contractions". Ph.D. thesis, UNB, 1973.

/10/ Winter, D.A. et al. "Measurement and characteristics of overall noise content in exercise electrocardiograms" Am. Heart J. September, 1967. Vol. 74. pp. 324-331.

/11/ Van Trees, H.L. Detection, Estimation and Modulation Theory, Part I, Wiley, U.S.A. 1968.

/12/ Burch, G. and T. Winsor. A Primer of Electrocardiography, Lea and Fabiger, U.S.A. 1972.

/13/ Hewlett-Packard Ltd. "Operating and Service Manual: 37224 Noise Generator". H/P, Scotland. 1971.

/14/ Morrison, R. Grounding and Shielding Techniques In Instrumentation, Wiley, U.S.A. 1967.